Published by Institute of Physics Publishing for SISSA
Received: June 6, 2005
Accepted: June 24, 2005
Published: August 17, 2005

Casimir scaling of domain wall tensions in the deconfined phase of $D = 3+1$ SU(N) gauge theories

Francis Bursa and Michael Teper

Rudolf Peierls Centre for Theoretical Physics, University of Oxford
1 Keble Road, Oxford OX1 3NP, U.K.
E-mail: f.bursa@physics.ox.ac.uk, m.teper1@physics.oxford.ac.uk

Abstract: We perform lattice calculations of the spatial 't Hooft k-string tensions, $\tilde{\sigma}_k$, in the deconfined phase of SU(N) gauge theories for $N = 2, 3, 4, 6$. These equal (up to a factor of T) the surface tensions of the domain walls between the corresponding (euclidean) deconfined phases. For $T \gg T_c$ our results match on to the known perturbative result, which exhibits Casimir Scaling, $\tilde{\sigma}_k \propto k(N-k)$. At lower T the coupling becomes stronger and, not surprisingly, our calculations show large deviations from the perturbative T-dependence. Despite this we find that the behaviour $\partial\tilde{\sigma}_k/\partial T \propto k(N-k)$ persists very accurately down to temperatures very close to T_c. Thus the Casimir Scaling of the 't Hooft tension appears to be a 'universal' feature that is more general than its appearance in the low order high-T perturbative calculation. We observe the 'wetting' of these k-walls at $T \simeq T_c$ and the (almost inevitable) 'perfect wetting' of the $k = N/2$ domain wall. Our calculations show that as $T \to T_c$ the magnitude of $\tilde{\sigma}_k(T)$ decreases rapidly. This suggests the existence of a (would-be) 't Hooft string condensation transition at some temperature $T_{\tilde{H}}$ which is close to but below T_c. We speculate on the 'dual' relationship between this and the (would-be) confining string condensation at the Hagedorn temperature T_H that is close to but above T_c.

Keywords: 1/N Expansion, Lattice Gauge Field Theories, Confinement.

JHEP08(2005)060

© SISSA 2005 http://jhep.sissa.it/archive/papers/jhep082005060.pdf/jhep082005060.pdf

Contents

JHEP08(2005)060

1. Introduction

In the euclidean formulation of SU(N) gauge theories at finite temperature T, deconfinement at $T = T_c$ is associated with the spontaneous breaking of a Z_N centre symmetry. This implies the existence of N degenerate phases for $T \geq T_c$ in our euclidean box. When such phases co-exist they are separated by domain walls. The tension of these domain walls is equal, up to a factor of T, to the spatial 't Hooft string tension. This is an interesting dynamical quantity that, for $T \leq T_c$, is in principle related to confinement.

As $T \to \infty$ one has $g^2(T) \to 0$ [4] and so one can calculate the spatial 't Hooft tension in perturbation theory [1−3]. These calculations [2] show that this tension satisfies Casimir Scaling (to 2 loops). This is an intriguing result given that the usual confining string tension between static sources is also known to satisfy Casimir Scaling to quite a good approximation [6−8]. Clearly it would be interesting to know whether the high T Casimir

Scaling that is characteristic of low order perturbation theory, persists to lower values of T where the coupling becomes strong and non-perturbative effects should be important. In particular it would be interesting to know what happens at $T \simeq T_c$ where one can imagine making contact with the confining phase.

In this paper we answer this question using numerical lattice techniques applied to SU(2), SU(3), SU(4) and SU(6) gauge theories. The plan of the paper is as follows. In section 2.1 we discuss in more detail the theoretical background to this problem. We then provide a summary of our lattice setup in section 2.2. In section 2.3 we describe how we can impose the existence of a domain wall by using twisted boundary conditions and then, in section 2.4, we describe how we can calculate (the derivative of) the surface tension from the average action. In section 2.5 we give the high-T prediction for the profile of the domain wall and describe how we obtain this profile in our lattice calculation. We complete section 2 with a discussion of finite volume corrections in section 2.6 and of 'wetting' in section 2.7. We then move on in section 3 to our calculations. Section 3.1 contains our results on the k-wall tension and makes the comparison with perturbation theory. In section 3.2 we calculate the domain wall profiles and again compare with perturbation theory. In section 3.3 we look for the appearance of a layer of confining phase in the centre of the k-wall as $T \to T_c$, pointing out that one can use the pattern of 'wetting' to tell us something about the domain wall between confining and deconfining phases. We finish in section 3.4 with a conjecture about the existence of a dual to the usual string condensation 'Hagedorn' transition. Section 4 gives our conclusions.

While this work was in progress a paper appeared [9] that addresses some of the same questions that we do, using a novel lattice technique that allows the direct calculation of the tension (rather than its derivative, as in this paper). The calculations, for SU(4) at a fixed value of the lattice spacing, observe consistency with Casimir Scaling down to $T = 1.2T_c$ just as we do. However our calculations test the Casimir scaling formula more tightly, because we work with SU(6) as well as SU(4), and we vary the lattice spacing so that we can address the continuum limit to some extent. In addition our range of T extends much closer to T_c.

2. Preliminaries

2.1 Background

As we remarked above, deconfinement in SU(N) gauge theories is associated with the spontaneous breaking of a Z_N centre symmetry. The symmetry arises from the fact that the partition function is unchanged if we impose that the time torus is periodic only up to a global gauge transformation belonging to the centre of the group, $z_k = \exp\{2i\pi k/N\} \in Z_N$. (The group element z_k contains a factor of the $N \times N$ unit matrix which we have suppressed. In fact it will be convenient to use the same notation, z_k, both for the phase factor and for the corresponding matrix. Which of the two we mean should always be clear from the context.) The obvious order parameter is the trace of the Polyakov loop, l_p, which is a closed Wilson line that winds once around the euclidean time torus and whose trace therefore acquires a factor of z_k under this symmetry transformation. In the confined

JHEP08(2005)060

phase the effective potential for the Polyakov loop trace averaged over the volume, $\bar{l}_p$, has its minimum at $\bar{l}_p = 0$ and so the symmetry is explicit. In the deconfined phase the minimum is at $\bar{l}_p \neq 0$ and so the symmetry tells us that there are N degenerate minima: the symmetry is spontaneously broken and there are N possible deconfined phases. If $\bar{l}_p \propto z_k$ we label the deconfined phase by k. When two of these deconfined phases, k_1 and k_2 say, co-exist they will be separated by a domain wall whose surface tension σ_W^k will depend on $k = k_1 - k_2$, as well as on N and T. At high T the coupling on the relevant length scale, $g^2(T)$, becomes small and one can calculate the domain wall surface tension in perturbation theory. To two loops one finds

$$\sigma_W^k = k(N-k)\frac{4\pi^2}{3\sqrt{3}}\frac{T^3}{\sqrt{g^2(T)N}}\{1 - \tilde{c}_2 g^2(T)N\} \tag{2.1}$$

where $\tilde{c}_2 \simeq 0.09$. (While the precise value of $\tilde{c}_2$ depends on the coupling scheme used [1], there appears to be only a $\sim 10\%$ variation between physically reasonable schemes.) The recently calculated 3-loop contribution [2] turns out to be negligible and so we do not include it here. The spatial 't Hooft string tension (see below) is related to the wall tension by

$$\tilde{\sigma}_k = \frac{\sigma_W^k}{T}. \tag{2.2}$$

(We use this notation because σ_k usually denotes the Wilson-loop k-string tension.)

The factor of T^3 in eq. (2.1) follows from dimensional analysis once T is large enough for it to be the only relevant scale, and to two loops σ_W^k is only a function of the 't Hooft coupling $\lambda \equiv g^2 N$ [1, 2]. The leading dependence on the coupling is $1/g$ rather than $1/g^2$ because there are no semiclassical domain walls: they are stabilised at one-loop. Although one might worry about the infrared divergences that eventually obstruct the perturbation expansion, numerical tests in 2+1 dimensions have shown that the lowest order perturbative calculations are remarkably accurate at all temperatures as long as they are not very close to T_c. Of course, as we reduce T we increase $g^2(T)$ and at some point the perturbative expansion becomes unreliable. For example if we use the 1-loop perturbative expression for the Debye screening mass, $m_D = T\sqrt{g^2(T)N/3}$ [4], and equate it to the lattice values calculated in [5] then we would find

$$g^2(T)N \sim 7.5\,, \qquad T \sim 2T_c \tag{2.3}$$

at which point the 2-loop correction in eq. (2.1) becomes $\sim 60\%$ of the 1-loop value and it is clear that we are past the point where we can be confident in perturbation theory (and indeed in the reliability of the calculation of m_D). At these values of T numerical calculations are the only unambiguous means of determining the physics.

The factor $k(N-k)$ in eq. (2.1) is the k dependence of the Casimir, $\mathrm{Tr}_{\mathcal{R}}\, T^a T^a$, when the represention $\mathcal{R}$ is the totally antisymmetric representation of a product of k fundamentals of SU(N). Thus it is the factor one obtains when calculating the Coulomb interaction between sources in such a representation. In D=1+1 SU(N) gauge theories, the tension of the confining k-string that emanates from such a source has precisely this dependence. In

JHEP08(2005)060

fact there are old speculations that this 'Casimir Scaling' holds in D=3+1 and numerical calculations show that it is in fact a good (but not exact) approximation to such k-string tensions — and an even better one in D=2+1 A question we will try to answer in this paper is whether the Casimir Scaling in eq. (2.1), which is an outcome of the low-order perturbative calculation, survives at very much lower T where perturbation theory becomes a manifestly poor approximation. This non-perturbative question will be addressed using numerical lattice techniques.

What connects this question to the role of Casimir Scaling in confinement, is that these domain walls are closely related to the centre vortices that provide a possible mechanism for confinement. Such a vortex will disorder any Wilson loop that encircles it, and the same for appropriate pairs of Polyakov loops. (We temporarily locate our discussion in the more easily visualisable case of D=2+1 [3].) At low T, in the confined phase, one postulates a condensate of such vortices, and a simple statistical calculation (see e.g. [13]) shows how this leads to linear confinement. Since the Wilson loops are in a euclidean space-time plane, the vortex cross-section will be in the same plane. As the euclidean time extent is reduced so as to increase T, at some point the vortex core is squeezed by the short temporal direction and becomes periodic in time. At this point one can no longer find a Wilson loop that encircle the vortex, but it will still disorder Polyakov loops that it separates. This co-incides with the onset of the deconfined phase, which is a 'Higgs' phase for these vortices, in which they become real, 'massive' objects. They are now precisely the domain walls which separate deconfined phases characterised by different Polyakov loop expectation values. The domain walls/vortices we discuss wind around a spatial torus. However they could equally well be of finite length, ending on appropriate Z_N monopoles [14]. Since the vortex cross-section is in a space-time plane, these monopoles will have world-lines in an orthogonal spatial direction (returning to D=3+1). They form the boundary of a spatial 't Hooft loop, and the domain wall tension is just the corresponding string tension (multiplied by T). Where this tension is non-zero, e.g. for $T > T_c$, these loops are not condensed. If however their tensions exhibit Casimir Scaling all the way down to T_c, where they might condense, then this may provide an extra ingredient in our (hopefully) growing understanding of confinement.

As an aside, we remark that although these domain walls certainly feature in the 4-dimensional euclidean field theory, they almost certainly do not entail real domain walls in the gauge theory at finite T. This has no implications for the calculations described herein. (A physical manifestation of these walls is described at the end of section 2.3.)

2.2 Lattice setup

We discretise euclidean space-time to a periodic hypercubic lattice. The lattice spacing is a and the lattice size, in lattice units, is L_μ in the $\mu = 0, 1, 2, 3$ directions. We choose the $\mu = 0$ direction as the short euclidean time direction that generates our temperature:

$$T = \frac{1}{aL_0} \,. \tag{2.4}$$

We will typically choose $L_1 = L_2$ and place the domain wall to span the $L_1 \times L_2$ torus. Typically $L_3 \gg L_1$ since it will need to contain 1 or 2 domain walls separating regions in two phases. In addition, for thermodynamics to be applicable, we need $aL_1, aL_2 \gg 1/T$.

JHEP08(2005)060

The fields are SU(N) matrices, U_l, on each link l of the lattice. (We sometimes label U_l more explicitly as $U_\mu(n)$ where μ is the direction of the link and $n = \{n_0, \vec{n}\}$ is the site from which it emanates.) We label the elementary squares (plaquettes) of the lattice by p and the ordered product of link matrices around the boundary of p by U_p. The partition function is then

$$Z = \int \prod_l dU_l e^{-\beta S} \tag{2.5}$$

and we use the plaquette action

$$S = \sum_p \left\{ 1 - \frac{1}{N} \mathrm{Re}\,\mathrm{Tr}\, U_p \right\}. \tag{2.6}$$

Analysing the continuum limit of this path integral, one finds that

$$\beta = \frac{2N}{g^2} \equiv \frac{2N}{g_L^2(a)} \tag{2.7}$$

where we have used the fact that g^2 is a lattice bare coupling to write it as some lattice scheme running coupling, g_L, on the length scale a. To approach the $N \to \infty$ limit smoothly, we need to keep fixed the 't Hooft coupling

$$\lambda(l) \equiv g^2(l)N \tag{2.8}$$

(where l is fixed in units of some well behaved quantity such as the mass gap) and so it is useful to define the 't Hooft inverse coupling

$$\gamma \equiv \frac{\beta}{2N^2} = \frac{1}{g_L^2(a)N}. \tag{2.9}$$

If we keep γ fixed as we take $N \to \infty$ then we ensure that a remains fixed in physical units for large enough N. (See figure1 of [5] for an explicit lattice demonstration of this.)

2.3 Imposing domain walls

Our order parameter will be based on the Polyakov loop

$$l_p(\vec{n}) = \frac{1}{N} \mathrm{Tr} \prod_{n_0=1}^{L_0} U_0(n_0, \vec{n}). \tag{2.10}$$

Consider the transformation where one multiplies all timelike link matrices at some fixed $n_0 = n_0'$ by a non-trivial element of the centre of SU(N), $z_k = e^{2\pi i \frac{k}{N}} \in Z_N$:

$$U_0(n_0 = n_0', \vec{n}) \longrightarrow z_k U_0(n_0 = n_0', \vec{n}) \qquad \forall \vec{n}. \tag{2.11}$$

A plaquette involving one such link matrix will necessarily involve the conjugate of a second and the centre factors will cancel, $z_k {z_k}^\dagger = 1$ so the plaquette remains unchanged. Since the measure is also unchanged, such a field has the same probability as the original field and we have a corresponding Z_N symmetry. A winding operator such as the Polyakov

JHEP08(2005)060

loop in eq. (2.10) will change under the symmetry transformation: $l_p \to z_k l_p$. It therefore provides an order parameter for the spontaneous breaking of the symmetry. In the confined phase where $\langle l_p \rangle = 0$ the symmetry is explicit, but in the deconfined phase where $\langle l_p \rangle \neq 0$ it is spontaneously broken with N degenerate phases in which $\langle l_p \rangle = z_k c(\beta)$ where $c(\beta)$ is a real-valued renormalisation factor. Such phases can co-exist at any $T \geq T_c$ and in that case they will be separated by domain walls. If the order parameter in the two phases differs by a factor z_k we shall refer to the domain wall as a k-wall. The domain wall may, for example, extend right across the 1-torus and 2-torus, and its world volume will wrap around the time torus. In such a case periodicity in x_3 means there must be at least two walls. Since the Polyakov loops on either side of the domain wall differ by some factor $z_k \in Z_N$, we see that the wall disorders Polyakov loops. Although we cannot encircle the wall with a Wilson loop in the (3,0)-plane, since the wall wraps right around the time torus, if we could then the Wilson loop would acquire a factor z_k as well. Thus, as remarked earlier, the domain wall is nothing but a spatial 't Hooft disordering loop in the (1,2)-plane, that has been squashed in the short temporal direction. We describe it as squashed because the size in the x_3-direction, where it is not squashed, is of the order of the inverse Debye mass

$$\frac{1}{m_D} \overset{T\to\infty}{=} \frac{1}{T}\sqrt{\frac{3}{g^2(T)N}} \gg \frac{1}{T} = aL_0 \tag{2.12}$$

to leading order in perturbation theory [4].

To study a k-wall we 'twist' the action in eq. (2.6) so as to enforce the presence of a single domain wall. The twisted action is defined by

$$S_k = \sum_p \left(1 - \frac{1}{N} \operatorname{Re} \operatorname{Tr}\{z(p) U_p\}\right). \tag{2.13}$$

where $z(p) = 1$ for all plaquettes except

$$z(p = \{\mu\nu, x_\mu\}) = z_k = e^{2\pi i \frac{k}{N}} \qquad \mu\nu = 03\,; \quad x_0 = x_0{}', \quad x_3 = x_3{}', \quad x_{1,2} = 1, \ldots, L_{1,2}\,. \tag{2.14}$$

That is to say, the plaquettes in the (0,3)-plane that are at the fixed values $x_0 = x_0{}'$ and $x_3 = x_3{}'$ and at all values of x_1 and x_2 are multiplied by $z_k \in Z_N$. This is a plane of plaquettes that wraps around the 1 and 2-tori at $x_0 = x_0{}'$ and $x_3 = x_3{}'$. Although the plane appears to be in a particular location this is an illusion. We can move it and deform it by redefinitions $U_l \to z_k U_l$ of suitable subsets of links. It is clear from considering such redefinitions that the Polyakov loops on either side of such a plane of twisted plaquettes will differ by a factor of z_k. Periodicity in x_3 then demands that at some x_3 the Polyakov loop must suffer a compensating factor of $z_k{}^\dagger$ so as to return to its original value. This requires an interface — a domain wall. Thus using such a twisted action we ensure that in the deconfined phase each configuration possesses at least one domain wall. This provides a convenient way to study different k-walls corresponding to different choices of k in eq. (2.13).

We will not discuss the interpretation of these walls in any detail, and instead refer the reader to [3, 15] for a more explicit discussion in the readily visualisable context of D=2+1, and to [16] for a more general theoretical review. Here we content ourselves with

JHEP08(2005)060

a few remarks for orientation. A finite line of twisted plaquettes enforces the presence of a Z_N Dirac string so that we have Z_N monopoles at the ends of the line [14]. The return flux between the monopoles is a centre vortex. A plane of such plaquettes thus corresponds to a 'dual' Wilson loop where a centre monopole propagates around the perimeter of the loop. There is now a vortex sheet that also ends on the perimeter of the loop. In our construction the loop is spacelike and we then extend the plane of twisted plaquettes right around the corresponding spatial two-torus, so that the boundary disappears and the vortex sheet, which now wraps around the two-torus, becomes decoupled in position from the centre Dirac sheet. Nonetheless the presence of the latter enforces the presence of the former. One may regard the plane of twisted plaquettes as effectively constituting an ultraviolet k-wall at zero cost. In the picture where vortex sheets are degrees of freedom relevant to confinement in the euclidean theory at $T = 0$ [16], the idea is that a closed k-vortex sheet can 'thread' a Wilson loop (just as a vortex loop would do in $D = 2 + 1$) and the Wilson loop then acquires a factor z_k. A condensate of such loops then leads to an area decay and linear confinement. These vortex sheets will in general close upon themselves rather than around the (infinite) torus. Our periodic construction is a device to impose the presence of a vortex sheet so that we can study it. In the deconfined phase such a spacelike vortex sheet is squashed by the short euclidean time direction so that it also extends around the time torus. And simultaneously the vortex sheet becomes real just as a 't Hooft-Polyakov monopole becomes real in the Higgs phase of the Georgi-Glashow model. It is in this phase that we can study it in the hope that what we learn will eventually have some bearing on confinement.

Finally we remark that this whole discussion becomes more transparent if we perform a cyclic relabelling of our co-ordinates, $x_o \to x_1$ etc., so that we have a sytem at low $T = 1/aL_3 \ll T_c$ but on a spatial three-torus where one of the tori is very short. In this case our Z_N monopole sources are timelike and the dual 't Hooft loop is in a space-time plane. The 't Hooft loop is imposed by the sheet of twisted plaquettes which generate the monopole Dirac sheet. It is now the short spatial torus that squashes the return flux between the monopoles. If we make the sheet of twisted plaquettes periodic in both directions then the squashed return flux manifests itself as a domain wall separating two phases in which the Polyakov loop around the short spatial torus has non-zero vacuum expectation values that differ by a factor of z_k between the two phases. This relabelled description has the advantage that it corresponds to real $T \simeq 0$ physics on such a spatial volume, in contrast to the original description which (for subtle reasons) does not imply the existence of real domain walls in high-T gauge theories.

2.4 Domain wall tension

Let us calculate the average action with and without a k-twist as defined above. Then, on a lattice that is of fixed size in lattice units,

$$\Delta S_k \equiv \langle S_k \rangle - \langle S_0 \rangle = \frac{\partial \ln Z_0}{\partial \beta} - \frac{\partial \ln Z_k}{\partial \beta} = \frac{\partial}{\partial \beta} \frac{F_k - F_0}{T} = \frac{\partial}{\partial \beta} \frac{\sigma_W^k A}{T} \tag{2.15}$$

where σ_W^k is the surface tension (energy per unit area) of the domain wall and $A = a^2 L_1 L_2$

JHEP08(2005)060

is its area. We assume the spatial dimensions are large enough that finite volume corrections are negligible. (We will of course need to check that this is so for our particular calculations.)

We see from eq. (2.1) that we expect

$$\Delta S_k = \frac{\partial}{\partial \beta}\frac{\sigma_W^k A}{T} \overset{T\to\infty}{=} \alpha(L_0)\frac{k(N-k)}{\sqrt{N}}\frac{4\pi^2}{3\sqrt{3}}\frac{L_1 L_2}{L_0^2}\frac{\partial}{\partial\beta}\frac{1}{g(T)} \tag{2.16}$$

when $T = 1/a(\beta)L_0$ is large enough that leading order perturbation theory is accurate. The additional factor of $\alpha(L_0)$ contains the $O(a^2T^2) = O(1/L_0^2)$ lattice correction to the continuum formula in eq. (2.1). We have obtained it by a numerical evaluation of the (non-closed) analytic expression given in [3] and the values are listed in table 1 for a range of aT. The calculations in this paper will be for $L_0 = 4, 5$ where the correction is modest.

L_0	$\alpha(L_0)$
∞	1
6	1.060
5	1.098
4	1.170
3	1.294
2	1.423

Table 1: Lattice correction to perturbative expression for σ_W^k.

To compare the perturbative expression in eq. (2.16) with our calculated values of ΔS_k we need to know the coupling $g^2(T)$ in terms of $g_L^2(a)$ and hence β. The simplest choice is obtained by asserting that to leading order the scale and distinction between running couplings is irrelevant, so we can use $g^2(T) \overset{lo}{=} g_L^2(a)$ and then

$$\frac{\Delta S_k}{L_1 L_2} \overset{T\to\infty}{=} \alpha(L_0)\frac{2\pi^2}{3\sqrt{6}}\frac{k(N-k)}{N}\frac{1}{L_0^2}\frac{1}{\sqrt{\beta}}\,. \tag{2.17}$$

In practice this is too crude. It is well known that $g_L^2(a)$ is a bad running coupling in that it has very large higher order corrections, so that it is only at unattainably asymptotic T that we could be confident of eq. (2.17) holding. The simplest, if partial, remedy is mean field improvement [17]

$$\beta_I = \beta \times \left\langle \frac{1}{N}\,\mathrm{Tr}\,U_p \right\rangle = \frac{2N}{g_I^2(a)}\,. \tag{2.18}$$

If we replace $g^2(T)$ in eq. (2.16) by $g_I^2(a)$ then we obtain

$$\begin{aligned}\frac{\Delta S_k}{L_1 L_2} &\overset{\text{1-loop}}{=} \alpha(L_0)\frac{2\pi^2}{3\sqrt{6}}\frac{k(N-k)}{N}\frac{1}{L_0^2}\frac{1}{\sqrt{\beta_I}}\left\{1+\beta\frac{\partial}{\partial\beta}\right\}\left\langle\frac{1}{N}\,\mathrm{Tr}\,U_p\right\rangle \\ &\simeq \alpha(L_0)\frac{2\pi^2}{3\sqrt{6}}\frac{k(N-k)}{N}\frac{1}{L_0^2}\frac{1}{\sqrt{\beta_I}}\end{aligned} \tag{2.19}$$

where the difference between the second line and the first is $O(1/\beta^{\frac{5}{2}})$ and is therefore negligible even to 2-loop order. (If we use the expansion to $O(\beta^{-8})$ obtained in [18] for the average plaquette, we see that even at our maximum value of a, corresponding to $a = 1/4T_c$, the numerical correction is no more than $\sim 17\%$.) In a similar way we obtain from eq. (2.1)

$$\Delta S_k \overset{\text{2-loop}}{=} \Delta S_k^{\text{1-loop}} \times \left\{1 + \frac{2\tilde{c}_2 N^2}{\alpha(L_0)\beta_I}\right\}. \tag{2.20}$$

We do not have a calculation of the lattice correction for the 2-loop term so we use no correc-

JHEP08(2005)060

tion in that case. The error from this should be small. The expressions in eqs. (2.19), (2.20) are what we shall usually use when making comparisons between perturbation theory and our lattice results.

There still remains the ambiguity associated with the scale T at which g_I^2 should be evaluated. Although, as we remarked above, the scale is irrelevant at one loop, this is really a formal statement. The point is that with a reasonable coupling, using an appropriate scale is the best way to ensure that higher order corrections are likely to be small. Of course, for $L_0 = 4, 5$ plausible scales such as πT and $2\pi T$ are numerically close to $1/a$, so it may be that using $g_I^2(a)$ for $g^2(T)$ is reasonable. However, it would be useful to have some estimate of how eq. (2.19) changes if we use the scale aL_0, say, rather than a in g^2. Near T_c this is a large spatial scale and so we need to use a lattice coupling scheme that we can have real confidence in. For this purpose we shall use the Schrödinger functional running coupling defined and calculated in [19]. We shall leave the detailed discussion and calculation to the appropriate point in section 3.

2.5 Domain wall profile

In addition to calculating the surface tension of the k-wall as described above, we can also calculate how the average Polyakov loop varies as one passes from one vacuum to the other through the domain wall, just as was done for the D=2+1 SU(2) case in [3].

Suppose the k-wall spans the $(1, 2)$ torus and is centered at $z = 0$ where $z \in (-\infty, +\infty)$ and we use continuum variables. Suppose the Polyakov loop satisfies

$$\bar{l}_p(z = -\infty) = 1\,; \qquad \bar{l}_p(z = +\infty) = e^{2\pi i \frac{k}{N}}\,. \tag{2.21}$$

Then to leading order in perturbation theory one finds [1]

$$\bar{l}_p(z) = \frac{1}{N}\,\mathrm{Tr}\, e^{2\pi i \frac{q(z)}{N} Y_k} \tag{2.22}$$

where Y_k is a diagonal matrix with $\{Y_k\}_{ii} = k$ for $i = 1, \ldots, N - k$ and $\{Y_k\}_{ii} = k - N$ for $i = N - k + 1, \ldots, N$ and $q(z)$ is a function that is independent of k. It is obtained from a one-loop effective potential calculation for the Polyakov loop [1, 3] which leads to

$$q(z) = \frac{e^{\sqrt{\frac{g^2 N}{3}}Tz}}{1 + e^{\sqrt{\frac{g^2 N}{3}}Tz}}\,. \tag{2.23}$$

Eqs. (2.22), (2.23) provide the 1-loop perturbative result for the domain wall profile for all k and N.

To compare this with our lattice calculations we have to choose a coupling $g^2(T)$ and, just as for the surface tension, we choose to use the coupling $g_I^2(a)$ defined in eq. (2.18). In addition the average Polyakov loop in the deconfined phase does not have unit length, but rather

$$|\langle \bar{l}_p \rangle| = c(\beta)\,. \tag{2.24}$$

This can be interpreted as the self-energy correction to the static source and is dominated by ultra-violet fluctuations which are insensitive to which phase we are in. Thus if we

JHEP08(2005)060

want to compare to the numerically calculated Polyakov loop we can simply renormalise the predicted Polyakov loop by a constant factor at all z

$$\bar{l}_p(z) \to c(\beta)\bar{l}_p(z) \tag{2.25}$$

where $c(\beta)$ can be determined from field configurations that are in a pure phase (and will depend on N as well as on β). In principle we could obtain lattice corrections to eqs. (2.22), (2.23) analogous to the factor $\alpha(L_0)$ for the surface tension. However we expect these to be small and so we neglect them. Thus eqs. (2.22), (2.23), (2.18), (2.25) provide the 1-loop perturbative result for the domain wall profile against which we shall compare our numerical lattice results.

2.6 Finite volume corrections

In principle the thermodynamic limit demands that we take $L_i \to \infty \,; i = 1, 2, 3$ at any fixed L_0 and β. In practice what this means is that we need to make these lengths large enough so that finite V corrections are small. We start with the most obvious.

2.6.1 Wall fluctuations

The fluctuations of the domain wall lead to corrections that are geometric and will not possess the k, N dependence of the domain wall tension — in exactly the same way as the Luscher correction to the mass of a confining string does not depend on the representation of the sources. Thus we want to make the wall area, $L_1 \times L_2$ large enough for these corrections to be negligible. The leading corrections are typically [20]

$$\begin{aligned} \frac{\delta\sigma_W^k}{\sigma_W^k} &\sim \frac{c}{L_0 L_1 L_2}\frac{1}{\sigma_W^k} \\ &\sim c\frac{3\sqrt{3}}{4\pi^2}\frac{\sqrt{g^2(T)N}}{k(N-k)}\frac{L_0^2}{L_1 L_2} \\ &< 0.01 \end{aligned} \tag{2.26}$$

where we have used the fact that $c \sim 1$ [20], eq. (2.3) as some guide to the largest value of $g^2(T)N$ and the fact that for our calculations we have $L_0 = 4, 5$ and $L_{1,2} = 20$. Thus with our choice of lattice sizes any such corrections will be very small.

2.6.2 Wall depth

We must also make sure that L_3 is long enough to accommodate the full depth of the domain wall. As pointed out in [3] this requires a much larger L_3 than one might naively expect. If we define the full width of the $L_3 = \infty$ wall, d_W, as extending between the points at which the Polyakov loop reaches two-thirds of its vacuum value, then the domain wall starts expanding once $aL_3 < 3d_W$ and completely disappears once $aL_3 \simeq 2d_W$. We therefore explicitly monitor the domain wall profile in each calculation and make sure that L_3 is large enough that there are no significant finite-L_3 corrections.

2.6.3 Spatial symmetry breaking

This correction is the most subtle and is typically relevant to calculations at very high T. In our case the problem arose when we performed calculations in SU(4) on $4 \times 12^2 \times 40$ and $4 \times 12^2 \times 60$ lattices at $\beta = 18, 20$ respectively. The latter β corresponds, very roughly, to $T \sim 1000T_c$ and we expected to obtain a good agreement with perturbation theory. However, while our result for the $k = 2$ domain wall was in agreement with eq. (2.19), the $k = 1$ result was about twice too large and even larger than the $k = 2$ result, which was clearly unphysical.

The cause of this phenomenon turns out to be a centre symmetry breaking in the spatial direction. That is to say, the average Polyakov loop in the $\mu = 1$ or $\mu = 2$ direction acquires a non-zero vacuum expectation value. In the case under discussion, the centre breaking occurred in the simulation with $k = 1$ twist but not for the untwisted $k = 0$ case. Thus the difference in actions was anomalous.

The practical cure, followed in the calculations in this paper, is obvious — calculate spatial Polyakov loops and choose the spatial lattice large enough to ensure that the symmetry breaking does not occur. For practical and theoretical reasons it would be interesting to understand this phenomenon sufficiently well to be able to estimate the spatial lattice size needed. This we now turn to.

At high T, if we perform a Fourier decomposition in x_0 of the SU(N) fields, we can keep just the lowest constant mode since there is an effective mass gap to the higher modes of $O(\pi T)$. The euclidean time integral in the action just gives $1/T$ and the action becomes that of a $D = 2 + 1$ gauge theory coupled to an adjoint scalar field (the remnant of the A_0 field). The coefficient in the action of the plaquette term is the corresponding D=2+1 inverse coupling, which we call g_3^2, and which clearly satisfies

$$\frac{1}{g_3^2} = \frac{1}{g^2(T)} \frac{1}{T} \quad \Longrightarrow \quad \beta_3 \equiv \frac{2N}{a g_3^2} \simeq \beta L_0 \tag{2.27}$$

at tree level. (An approximation that can be systematically improved upon). If we now neglect the massive adjoint scalar field (again an approximation that can be improved upon) we obtain a $D = 2+1$ SU(N) gauge theory on a $L_1 \times L_2 \times L_3$ lattice with the usual plaquette action. All this is the well-known phenomenon of dimensional reduction at high T. (See [21] for a recent discussion.)

Suppose for a moment that $L_2, L_3 \gg L_1$. Then as we increase β_3 this $D = 2 + 1$ SU(N) gauge theory will at some point deconfine and at this point the average Polyakov loop in the shorter x_1 direction (which plays the role of the euclidean time direction in the $D = 2 + 1$ system) acquires a non-zero expectation value. This is precisely the 'spatial symmetry breaking' in the parent $D = 3 + 1$ gauge theory that we discussed above. When will it occur? This is easy to estimate. Using eq. (2.27) we have a specific value of β_3 corresponding to given values of β and L_0. The string tension, $a^2\sigma$, can be obtained for any N and for any β_3 from the calculations in [22]. (It helps to know the average plaquette for the interpolation.) We now note that in $D = 2+1$ one finds $T_c \sim \sqrt{\sigma}$ [23]. (This is based on SU(2) and SU(3); calculations for all N are in progress [24].) Thus in the case cited above, with $\beta = 20$ and $L_0 = 4$ and $N = 4$, we have $\beta_3 \simeq 80$ which turns out to correspond

JHEP08(2005)060

to $a\sqrt{\sigma} \simeq 0.08$ [23] so that the critical value of L_1 will be $L_1^{crit} = 1/aT_c \sim 1/a\sqrt{\sigma} \sim 12$. Since in $D = 2+1$ one has $a\sqrt{\sigma} \propto 1/\beta_3$ at large β_3, the value of L_1^{crit} corresponding to $\beta = 18$ in the D=3+1 theory will not be very different. Finally, the fact that L_3 is finite and that $L_2 \ggg\!\!\!\!/\, L_1$ but rather $L_2 = L_1$ means that the transition is smeared in β_3 (and hence in β) and that it may occur for one of the two transverse directions chosen at random. Thus the observed scenario where on some lattices the transition occurs and on others it does not, is just what one expects. Using the above approach one can estimate the critical value of $L_{1,2}$ for any particular β and $L_0 \ll L_{1,2}$ and thus avoid the corresponding spatial symmetry breaking.

It is interesting to note that at high T in $D = 2+1$ there should be no such spatial symmetry breaking because the dimensionally reduced $D = 1+1$ gauge theory confines at all T. (The confining string cannot vibrate in one space dimension.) Indeed careful finite V studies in D=2+1 [3] have not observed any unexpected behaviour of the domain wall tension at very high T. It is perhaps over-familiarity with $D = 2+1$ that led us to be surprised by what occurs in $D = 3+1$.

2.7 Wetting at $T \simeq T_c$

Since the phase transition is first order for $N \geq 3$ one can have the confined phase as well as the various deconfined phases co-existing at $T = T_c$. We can always interpolate between any two deconfined phases by passing through the confined phase, and whether the system chooses to do so or not will depend on the relevant wall free energies, i.e surface tensions. A k-wall between two deconfined phases will be stable against breaking up into two confined-deconfined domain walls, with surface tension σ_{cd}, provided that

$$\sigma_W^k(T_c) < 2\sigma_{cd}(T_c)\,. \tag{2.28}$$

In this case it is only at some $T < T_c$ that the k-wall would split. Another possibility is

$$\sigma_W^k(T_c) = 2\sigma_{cd}(T_c)\,. \tag{2.29}$$

This corresponds to 'perfect wetting'. It has been conjectured [26] that this occurs in the SU(3) gauge theory, where there are only $k = 1$ walls. (See [9] for a recent discussion.) A third possibility is that the continuation from higher T would give

$$\sigma_W^k(T_c) > 2\sigma_{cd}(T_c)\,. \tag{2.30}$$

In that case there would be some critical value of T above T_c where a pair of confined-deconfined domain walls would have the same free energy and from there onwards, as $T \to T_c$, the k-wall will be on the $\sigma_W^k(T) = 2\sigma_{cd}(T)$ branch. (So that in practice the condition in eq. (2.29) will be satisfied.)

We recall that the confined and deconfined phases correspond to the $N+1$ degenerate minima of the effective action, calculated as a function of $\bar{l}_p$. The confined phase is at $\bar{l}_p = 0$ and the N deconfined phases at $\bar{l}_p = c(\beta)e^{2\pi ik/N} : k = 0, \ldots, N-1$. A domain wall between two phases is a tunnelling path between the corresponding minima that minimises the effective action. (A proper analysis, as in [1, 2] for very high T, needs to express the effective potential not just in terms of the trace of the Polyakov loop but in terms of its

JHEP08(2005)060

eigenvalues.) At high T it is enough to keep the effective potential and a term quadratic in derivatives [1, 2]. In this case one has the usual simple intuition about how tunnelling paths are determined by the potential. As $T = 1/aL_0$ decreases the coupling $g^2(T)$ increases and eq. (2.23) tells us that the domain wall will become thinner, $\propto 1/g(T)$, on the scale of $1/T$. This could imply that higher order derivative terms will become more important in the effective action. In reality however, as we shall see, the walls become thicker rather than thinner as $T \to T_c$, suggesting that the simple picture of a potential plus quadratic derivatives might remain reliable beyond its naive domain of validity.

If we increase T slightly away from T_c then the minimum at $\bar{l}_p = 0$ rises and the confining phase becomes metastable. If we keep increasing T then eventually this minimum ceases to play any role and we need only consider the N deconfined minima. At high T one can calculate these tunnelling paths in perturbation theory [1, 2] as summarised in section 2.5. For example, one finds that the $k = N/2$ domain wall that runs between the $k = 0$ and $k = N/2$ phases passes through $\bar{l}_p = 0$. In practice, as we shall see below, this behaviour persists all the way down to $T = T_c$. Given this we expect $\sigma_W^{k=N/2}(T_c) = 2\sigma_{cd}(T_c)$; i.e 'perfect wetting'. Indeed we expect this equality to hold at any T close enough to T_c for $\sigma_{cd}(T)$ to make sense. Thus we expect that at $T = T_c$ the $k = N/2$ wall will break up into two confined-deconfined walls. Since at T_c the confined and deconfined free energies are equal, these two walls can separate and rejoin.

As an aside we remark that the above scenario allows us to calculate T_c on arbitrarily large volumes, in contrast to the standard calculations such as in [5]. For example, direct tunnelling at $T = T_c$ from the confined to the deconfined phase on a lattice larger than $16^3 5$ will simply not occur in a SU(6) Monte Carlo calculation of feasible length [5]. The reason is the thermodynamic suppression of the large domain walls that occur as a necessary intermediate step in the tunnelling. Here, by contrast, our twisted boundary conditions enforce the presence of a k-wall that can have enough free energy to split into two confined-deconfined walls irrespective of how large is the volume. In this context β_c can be identified by the fact that the growth and shrinkage of the confined and deconfined sub-volumes follows an unbiased random walk. In principle this provides a practical technique for directly locating T_c on arbitrarily large volumes.

A $k \neq N/2$ domain wall, on the other hand, does not pass through $\bar{l}_p = 0$ at high T. Thus an alternative tunnelling path from the $k = 0$ to $K = N/2$ minima is not via $\bar{l}_p = 0$, but rather via the paths joining the sequence of minima $K = 0 \to 1 \to \cdots \to N/2$. While this is clearly a local minimum of the effective action, this minimum turns out to be sufficiently higher than the direct path through $\bar{l}_p = 0$ that it does not play a role in practice. More interesting is the reverse possibility: for tunnelling between the k and k' phases, there is a minimal path that first runs from the k minimum to $\bar{l}_p = 0$ (just like the first half of the $k = N/2$ domain wall) and then runs out from $\bar{l}_p = 0$ to the k' minimum. We would expect this to have an effective action equal (approximately) to that of the $k = N/2$ tunnelling path and thus to be too large to contribute at high T (where we know that we have paths that satisfy Casimir Scaling). However as T drops to and below T_c there will certainly be a point at which the path through $\bar{l}_p = 0$ comes to have a lower action than the path not through $\bar{l}_p = 0$. It could of course be that the shape of the

JHEP08(2005)060

effective potential also changes so that the latter path smoothly deforms into the former at $T \simeq T_c$. However our calculations (see below) suggest that what actually occurs is that there is a tunnelling from one kind of path to the other. So if Casimir Scaling persists all the way down to T_c, we expect that it will only be at some T below T_c that the $k = 1$ wall breaks up into two cd walls. In this sense we do not expect 'perfect wetting' for domain walls in SU(3), since these are necessarily $k = 1$.

The above remarks suggest a possible way of determining whether σ_{cd} is $O(N)$ or $O(N^2)$, something which direct calculations [5] have so far been unable to determine unambiguously. Since we have found that $\sigma^k_W(T)$ satifies Casimir Scaling very accurately down to $T \simeq 1.02T_c$, it is plausible to assume that it will continue to do so down to $T = T_c$. In that case the N-dependence is $\sigma^k_W(T_c) \propto k(N-k)$ and so $2\sigma_{cd} = \sigma_W^{k=N/2}(T_c) \propto N^2$. More generally by observing for which values of k and N the domain walls wet at $T = T_c$, one can imagine being able to pin down σ_{cd} quite accurately. The calculation in this paper does not have the range of k and N to make this a realistic goal, but we can at least attempt to gauge the potential of such a strategy.

3. Results

The strategy of our calculation is as follows. We first perform calculations of $k = 1$ and $k = 2$ domain walls in SU(4) at a very high temperature, $T \sim 1000T_c$, where we can expect our results to match perturbation theory quite precisely. We then repeat the calculations much closer to T_c, where perturbation theory is *à priori* no longer useful. We do so for $L_0 = 4$ and for $L_0 = 5$, so that at each T we have results at two values of a. i.e. $a = 1/4T$ and $a = 1/5T$. This allows us to make some statement about the continuum limit. We then perform calculations of $k = 1, 2, 3$ domain walls in SU(6), for $L_t = 5$, which together with the SU(4) results provide us accurate information on the full k and N dependence of the surface tension. As a check on the N-dependence of the low T behaviour of the $k = 1$ surface tension we also perform some SU(2) and SU(3) calculations.

We simultaneously calculate the domain wall profiles and compare them with perturbation theory. As $T \to T_c$ we look for the breakup of the k-wall into two confined-deconfined domain walls separated by a region of confining phase ('wetting' and 'perfect wetting'). In principle this provides a way to obtain information about the N-dependence of the corresponding surface tension, σ_{cd}.

Finally we list the values of β that correspond to $T = T_c$ for the calculations in this paper:

$$\beta_c = \begin{cases} 10.4865(3) - 0.067(7)/VT^3 : & L_0 = 4\,; \quad SU(4) \\ 10.6373(6) - 0.090(17)/VT^3 : & L_0 = 5\,; \quad SU(4) \\ 24.5139(24) - 0.112(19)/VT^3 : & L_0 = 5\,; \quad SU(6) \end{cases} \tag{3.1}$$

The last two values are taken from [5, 25] while the first is a calculation performed in this paper. Exhibiting the volume dependence allows us to correct for a finite volume shift, although in practice this will be completely negligible for us.

JHEP08(2005)060

N	β	L_0	L_3	$L_{1,2}$	Sweeps	β_I	T/T_c
2	2.4843	4	30	20	100000	1.6144	1.88
3	5.702	4	30	20	100000	3.159	1.02
3	6.013	4	30	20	100000	3.585	1.88
4	10.5	4	30	20	100000	5.644	1.02
4	11	4	30	20	100000	6.360	1.88
4	20	4	30	20	100000	15.954	~ 1000
4	10.654	5	30	20	68000	5.878	1.02
4	11.239	5	30	20	100000	6.654	1.88
6	24.545	5	30	20	20000	13.190	1.02
6	25.863	5	30	20	20000	15.019	1.88

Table 2: Parameters of the SU(N) calculations on $L_0 \times L_1 \times L_2 \times L_3$ lattices at the values of β shown. Also the number of Monte Carlo sweeps, the mean-field improved coupling β_I, and the value of T.

N	β	$\overline{u}_p$	$\overline{u}_p^{k=1}$	$\overline{u}_p^{k=2}$	$\overline{u}_p^{k=3}$
2	2.4843	0.6498239(90)	0.6493949(74)		
3	5.702	0.554069(23)	0.552153(51)		
3	6.013	0.5962242(67)	0.5958470(65)		
4	10.5	0.537515(16)	0.535272(39)	0.534541(39)	
4	11	0.5781191(54)	0.5778135(56)	0.5777084(57)	
4	20	0.7977065(13)	0.7976478(18)	0.7976278(15)	
4	10.654	0.551683(12)	0.550862(27)	0.550592(29)	
4	11.239	0.5920068(40)	0.5918633(45)	0.5918131(54)	
6	24.545	0.537364(17)	0.536822(22)	0.536423(25)	0.536236(27)
6	25.863	0.5807296(78)	0.5806203(71)	0.5805524(80)	0.5805399(85)

Table 3: Average plaquette values obtained in the calculation listed in table 2, for no twist and for $k = 1, 2, 3$ twists.

β	L^4	$a\sqrt{\sigma_{k=1}}$	$a\sqrt{\sigma_{k=2}}$	$\sigma_{k=2}/\sigma_{k=1}$	plaq
10.48	8^4	0.4300(21)	0.496(7)	1.331(20)	0.525301(54)
10.50	8^4	0.4170(16)	0.481(4)	1.331(12)	0.529210(50)

Table 4: Additional SU(4) calculations of the $k = 1$ and $k = 2$ string tensions and average plaquettes.

3.1 Surface tension

The parameters of our high statistics calculations are listed in table 2 and the corresponding values of the average plaquette are listed in table 3. We have deliberately chosen the values of β so that the values of T/T_c are closely matched across the various SU(N) groups. (For T_c we use the values in eq. (3.1) and for interpolations we use the the string tension values in [10] as well as the extra calculations listed in table 4. One can instead interpolate using the values of $\beta_c(L_0)$ in [5, 25] and this will give values of T/T_c that differ at the 1% level

JHEP08(2005)060

N	aT	k	Prediction	$\Delta S^k_w/L_xL_y$	$\Delta S^k_w/\Delta S^1_w$	CS	T/T_c
2	0.25	1	0.1042	0.3089(84)			1.88
3	0.25	1	0.1032	1.380(40)			1.02
3	0.25	1	0.0936	0.2716(67)			1.88
4	0.25	1	0.0867	1.615(30)			1.02
		2	0.1157	2.141(30)	1.326(29)	1.333	1.02
4	0.25	1	0.0791	0.2200(56)			1.88
		2	0.1055	0.2957(57)	1.344(31)	1.333	1.88
4	0.25	1	0.0421	0.0423(16)			~ 1000
		2	0.0561	0.0567(14)	1.341(49)	1.333	~ 1000
4	0.20	1	0.0514	0.739(27)			1.02
		2	0.0685	0.982(28)	1.329(56)	1.333	1.02
4	0.20	1	0.0467	0.1292(54)			1.88
		2	0.0622	0.1743(60)	1.350(57)	1.333	1.88
6	0.20	1	0.0381	0.488(25)			1.02
		2	0.0610	0.847(27)	1.74(9)	1.60	1.02
		3	0.0687	1.015(29)	2.08(10)	1.80	1.02
6	0.20	1	0.0345	0.098(9)			1.88
		2	0.0552	0.159(10)	1.62(14)	1.60	1.88
		3	0.0621	0.171(10)	1.74(15)	1.80	1.88

Table 5: Action differences from table 3 and their ratios, compared to perturbative and Casimir scaling predictions respectively.

from the ones we list.) These values, $T \simeq 1.88T_c$ and $T \simeq 1.02T_c$, take us very close to the deconfinement transition itself. In addition we have performed a calculation for SU(4) at a very large value of β, which corresponds to $T \sim 1000T_c$, where we expect to find good agreement with the perturbative result.

In table 5 we list the results of our calculations of ΔS^k_W. We also list the 2-loop perturbative expectation obtained from eq. (2.20), using for $g^2(T)$ the mean-field improved coupling $g^2_I(a)$ defined in eq. (2.18).

Consider first the values of ΔS^k_W that we obtain in SU(4) at $\beta = 20$, which corresponds to $T \sim 1000T_c$. We observe excellent agreement with perturbation theory for both $k = 2$ and $k = 1$ walls. The ratio of the $k = 2$ and $k = 1$ values therefore exhibits Casimir Scaling, i.e. is $\propto k(N-k)$. At such a very high T all this is to be expected — but it provides a reassuring check on our calculations.

Moving on to the other SU(4) calculations with $aT = 1/L_0 = 1/4$, we observe that as $T \to T_c$ the value of ΔS^k_W grows much more rapidly than the perturbative prediction. Indeed at $T \simeq 1.02T_c$ the discrepancy is very large, a factor of ~ 18, and even at $T \simeq 1.88T_c$ it is a substantial factor ~ 3. This is essentially telling us that $\partial\sigma^k_W/\partial T$ becomes much larger than the low-order perturbative expectation as $T \to T_c$. Since at large T the domain wall tension tends to its perturbative value, what this implies is that $\sigma^k_W(T)$ is increasingly suppressed relative to its perturbative value, as we approach T_c. Later on in this section we shall provide an estimate of this suppression.

JHEP08(2005)060

Although we find that ΔS_W^k deviates strongly from low-order perturbation theory as T approaches T_c, we also see from table 5 that the ratio of $\Delta S_W^{k=2}$ to $\Delta S_W^{k=1}$ continues to satisfy Casimir Scaling, to a high precision, even down to $T \simeq 1.02T_c$. This is a remarkable and unexpected result.

All these calculations are at a fixed value of the lattice spacing in units of T, i.e. $aT = 1/4$. At this value of a we expect typical lattice spacing corrections to both the non-perturbative and perturbative calculations to be small but not negligible (see e.g. table 1). Nonetheless it would be useful to check that the effects we are seeing do not change significantly in the continuum limit. To obtain some control over that limit we repeat our calculations for $L_0 = 5$, i.e. $aT = 1/5$. The leading lattice corrections should be $O(a^2T^2)$ and so should be reduced by a factor $\sim 2/3$ when we go from $L_0 = 4$ to $L_0 = 5$. We see from table 5 that at $T \simeq 1.88T_c$ we observe a discrepancy with perturbation theory that is essentially identical to the one we saw at the coarser lattice spacing. Thus we can infer that this discrepancy is a continuum effect. For $T \simeq 1.02T_c$ the ratio to the perturbative result is ~ 15 for $L_0 = 5$ rather than the ~ 18 we saw for $L_0 = 4$, but since this ratio is varying very rapidly with T when we are this close to T_c, it is not clear whether this apparent variation with a is due to lattice spacing corrections or is due to a slight mismatch between the values of T/T_c at the two values of a. In any case it is clear that a large and growing mismatch with perturbation theory as $T \to T_c$ is a feature of the continuum theory. Nonetheless we see that the ratio of the ΔS_W^k continues to accurately satisfy Casimir Scaling when we decrease a, so that is also a property of the continuum theory.

We now turn to our SU(6) calculations. These have been performed for $L_0 = 5$ rather than $L_0 = 4$ so as to avoid the first order bulk transition [5] that separates the lattice strong and weak coupling regimes for $N \geq 5$. This and the fact that our statistics are smaller (the computational cost grows roughly $\propto N^3$) means that our results are significantly less precise than for SU(4). Nonetheless it is clear from table 5 that we observe at both values of T precisely the same discrepancy with perturbation theory as we saw for SU(4) at the same value of L_0. In addition the ΔS_W^k ratios continue to satisfy Casimir Scaling (albeit only at the 2σ level at $T \simeq 1.02T_c$). This and the fact that the discrepancy with perturbation theory is the same as for SU(4) tells us that the domain wall tension has no factors of k and N except for the Casimir scaling factor $k(N-k)$ and its dependence on the 't Hooft coupling, g^2N. (The latter follows from the fact that everything is only a function of T/T_c and that fixed T_c is obtained by keeping g^2N fixed at large-N [5].)

Finally we note in table 5 that our calculations of the SU(2) and SU(3) $k = 1$ domain wall tensions show a very similar discrepancy with perturbation theory. (The SU(2) transition is second order and this prevents us from performing reliable domain wall calculations at $T \simeq 1.02T_c$.) Thus the suppression of $\sigma_W^k(T)$ as $T \to T_c$ is largely independent of N.

To illustrate the above, we plot in figure 1 the values of $\Delta S_W^{k=1}$ for our $L_0 = 4$ SU(4) calculations, and compare to the two-loop perturbative expectation, eq. (2.17), using the mean-field improved coupling, β_I, as well as the unimproved lattice bare coupling β. (The fact that both the lattice and perturbative calculations exhibit Casimir Scaling means that we would obtain a very similar comparison in SU(6).) We see the growing discrepancy as $T \to T_c$ that was discussed above. We also see a substantial difference between the

JHEP08(2005)060

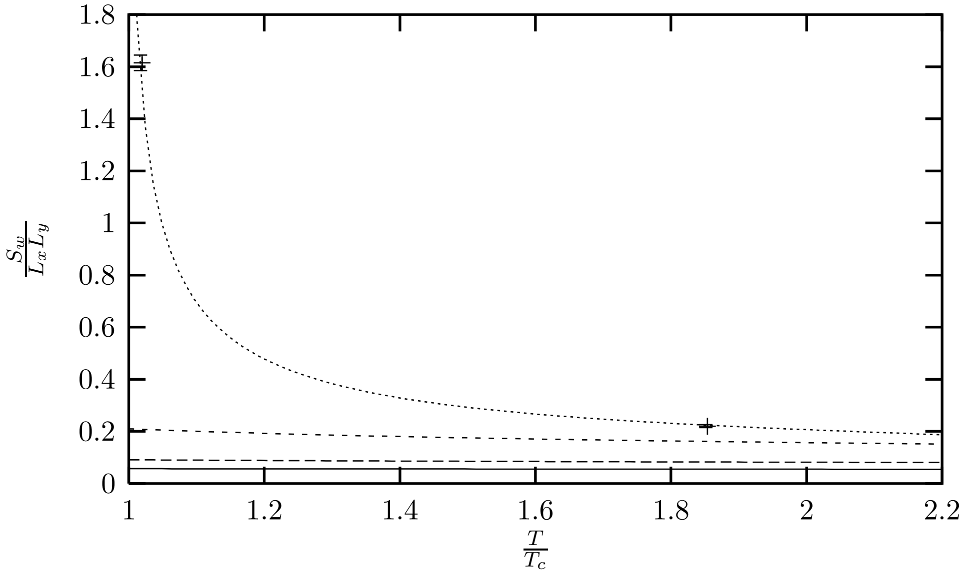

Figure 1: Action per unit area of the $k = 1$ domain wall in SU(4) with $aT = 0.25$. Monte Carlo values, $+$, compared with perturbation theory based on verious couplings: $g^2(a)$, solid line, $g_I^2(a)$, long dashed line, $g_{SF}^2(T)$, short dashed line. The dotted line is the interpolation in eq. (3.3).

two perturbative predictions. It is therefore relevant to ask how much of the observed discrepancy with perturbation theory might be due to the fact that our choice of coupling or scale is becoming inappropriate on the large distance scales associated with the limit $T \sim T_c$. To address this question we shall choose some standard 'good' coupling whose running has been evaluated down to low enough energy scales that we can extrapolate with some confidence to scales $\sim T_c$. (This approach is at best qualitative: a proper calculation would require us to redo every part of the calculation in whatever coupling scheme we use, and this (more formidable) calculation we do not attempt.) An example of such a coupling is the Schrödinger functional coupling whose running has been calculated non-perturbatively in [19]. In appendix A, we describe the evaluation of this coupling on the length scale $T^{-1} = aL_0$ and we show the result in figure 2. Note that the direct calculation [19] goes down to about $T \simeq 2T_c$ and from there onwards we extrapolate $g_{SF}^2(T)$ using the '3-loop' beta function calculated in [19]. We use this coupling to obtain ΔS_W^k and we show the result in figure 1. We see that while using this coupling reduces the discrepancy at $T \simeq 1.88T_c$, it it is still far from large enough to bridge the observed gap at $T \simeq 1.02T_c$. This suggests that for $T \to T_c$ the domain wall tension becomes increasingly dominated by non-perturbative physics.

Returning to the evidence for the Casimir Scaling of the k-wall tensions, we average our accurate SU(4) ratios for $aT = 0.20, 0.25$ giving

$$\frac{\Delta S_W^{k=2}}{\Delta S_W^{k=1}} = \begin{cases} 1.327(26) : & T \simeq 1.02T_c \\ 1.345(27) : & T \simeq 1.88T_c \\ 1.341(49) : & T \sim 1000T_c \\ 1.333\ldots : & \text{Casimir Scaling}\,. \end{cases} \tag{3.2}$$

JHEP08(2005)060

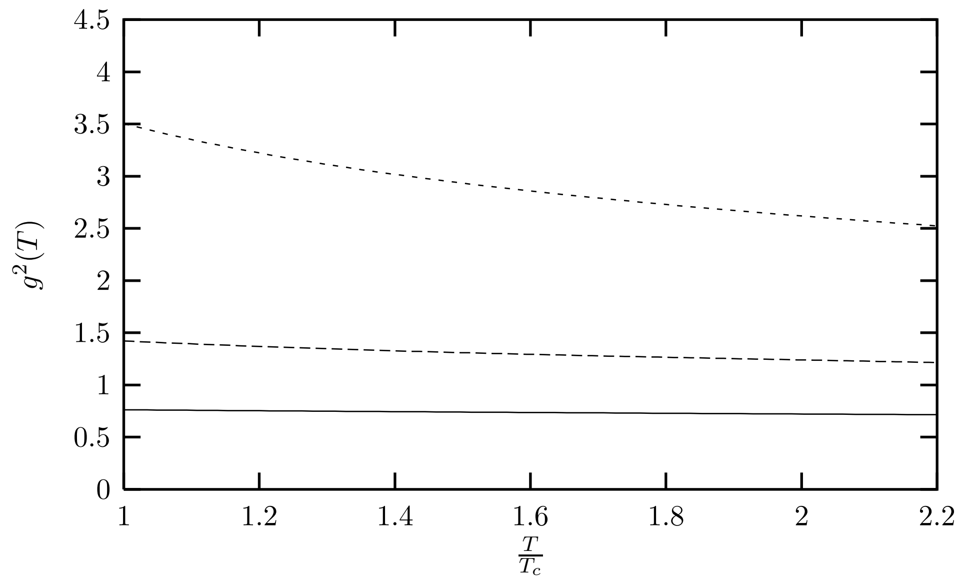

Figure 2: The running coupling $g^2(T)$ obtained from the lattice bare coupling (solid line), the mean field improved bare coupling (dashed line), and the Schrödinger functional coupling (short dashed line). All for SU(4) and $aT = 0.25$.

This (together with the results at $T/T_c = 2.3, 1.5, 1.2$ of [9]) provides impressively accurate evidence for the Casimir scaling of domain wall tensions (or 't Hooft string tensions) and their derivatives from $T = \infty$ all the way down to $T \simeq 1.02T_c$.

The fact that, when T decreases towards T_c, $\partial\sigma_W^k/\partial T$ increases more strongly than expected from perturbation theory, tells us that σ_W^k must decrease more rapidly than expected as $T \to T_c$. In principle we can calculate σ_W^k as a function of T by interpolating $\partial\sigma_W^k/\partial\beta$ in β and then integrating from large β, where it asymptotes to the perturbative value, down to the desired value of T. In practice our calculations are not dense enough in β to determine the interpolation unambiguously. (They were not intended for this purpose). Therefore the best we can do is to obtain a qualitative picture by assuming some functional form for $\partial\sigma_W^k/\partial\beta$ and fitting it to the few calculated values we have. Choosing the $L_0 = 4$ SU(4) calculation, we display in figure 1 our best fit to ΔS_W based on a simple modification of the one-loop formula to the k-wall free energy:

$$\frac{F_W^k}{L_1 L_2 T} = [1 \text{ loop}] + a\exp(-b\sqrt{\beta_I - \beta_{Ic}})\,. \tag{3.3}$$

(The fit is also constrained to go through the very large β value which is not shown in the figure.) Using this fit we then obtain the the T-dependence of σ_W^k shown in figure 3. We display the uncertainty that arises from the errors in the fitted parameters, but it is clear that we cannot reliably estimate the systematic error inherent in the choice of fitting function. However we can see from figure 1 that our interpolation is conservative in that, if anything, it errs on the side of minimising the value of $\partial\sigma_W/\partial T$ in the region $T \geq 1.02T_c$. We also show in figure 3 the two-loop perturbative prediction (using the improved lattice coupling). The qualitative picture is that σ_W^k is strongly suppressed at $T \leq 2T_c$, well below

JHEP08(2005)060

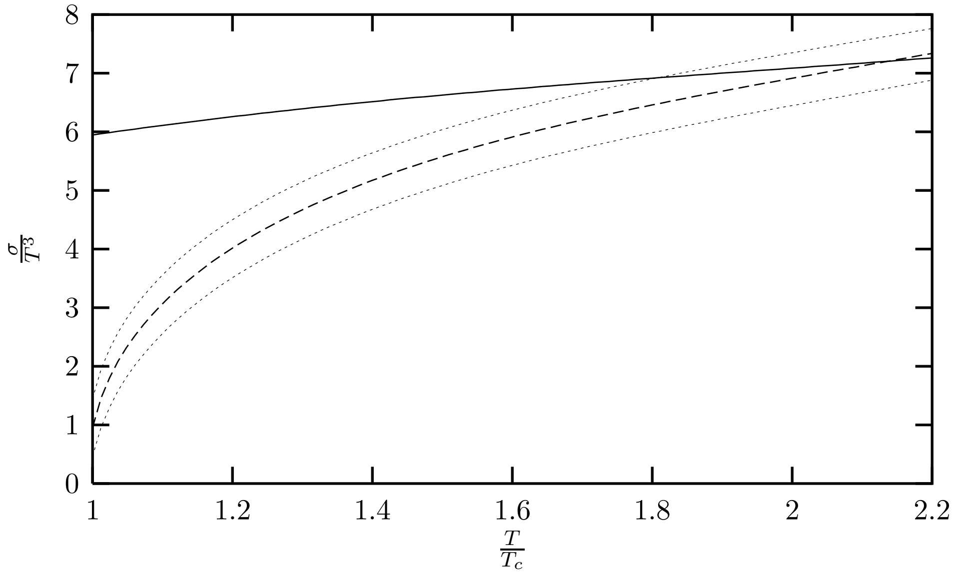

Figure 3: Surface tension in units of T, using the interpolation shown in figure 1. For comparison we show the 2-loop perturbative result using the mean field improved coupling. All for the $k = 1$ wall in SU(4).

the perturbative expectations, to the point of being close to zero at $T = T_c$. This is not inconsistent with our picture of these domain walls as being squashed but 'real' Z_N vortices that condense into the vacuum in the confined phase.

3.2 Profile

As described above, imposing suitable twisted boundary conditions in the deconfined phase ensures that each lattice field contains a single domain wall. (Assuming, as is always the case for us, that the thermal production of extra pairs of domain walls is completely negligible.) If we average the Polyakov loop over the transverse co-ordinates we obtain the profile $\bar{l}_p(x_3)$. This profile maps the interval $x_3 \in [0, L-1]$ to a line in the complex plane corresponding to the values that $\bar{l}_p(x_3)$ takes as x_3 runs over the x_3-torus. This line can be directly compared to the perturbative one loop prediction in eqs. (2.21)–(2.25). Note that this comparison is independent of the choice of $g^2(T)$. (As we see from eq. (2.23) the value of the coupling determines the rate at which $\bar{l}_p$ runs along the line in the complex plane, as x_3 is varied, but not the actual locus of the line.) Thus any disagreement between calculated and perturbative loci cannot be put down to the use of an inappropriate coupling or scale.

In figure 4 and figure 5 we compare the one-loop perturbative prediction for the SU(4) $k = 1$ locus, to what we obtain at $T \simeq 1.88T_c$ and at $T \simeq 1.02T_c$ respectively, in our lattice calculations. Plotting the fluctuating locus for each lattice field would clutter the plot so what we show is an average line. These results are also characteristic of what we observe for $L_0 = 5$ and for SU(6) and other k. What we observe is not only excellent agreement at the very highest T (not shown here), but also, from figure 4, that the agreement remains

JHEP08(2005)060

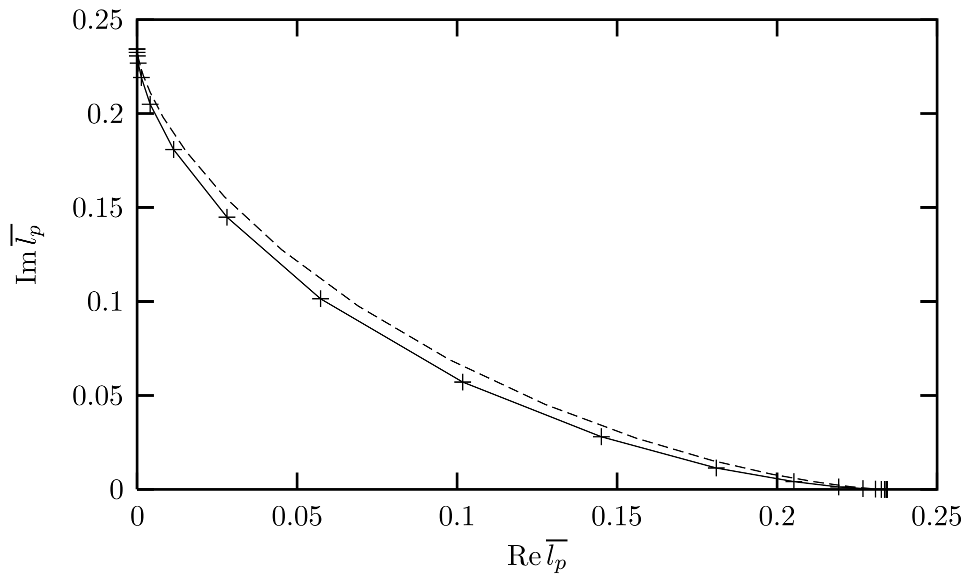

Figure 4: The values in the complex plane taken by the Polyakov loop for $x_3 \in [0, L-1]$, for the $k = 1$ wall in SU(4) with $aT = 0.25$ and $T \simeq 1.88T_c$. Dashed line is one-loop perturbation theory.

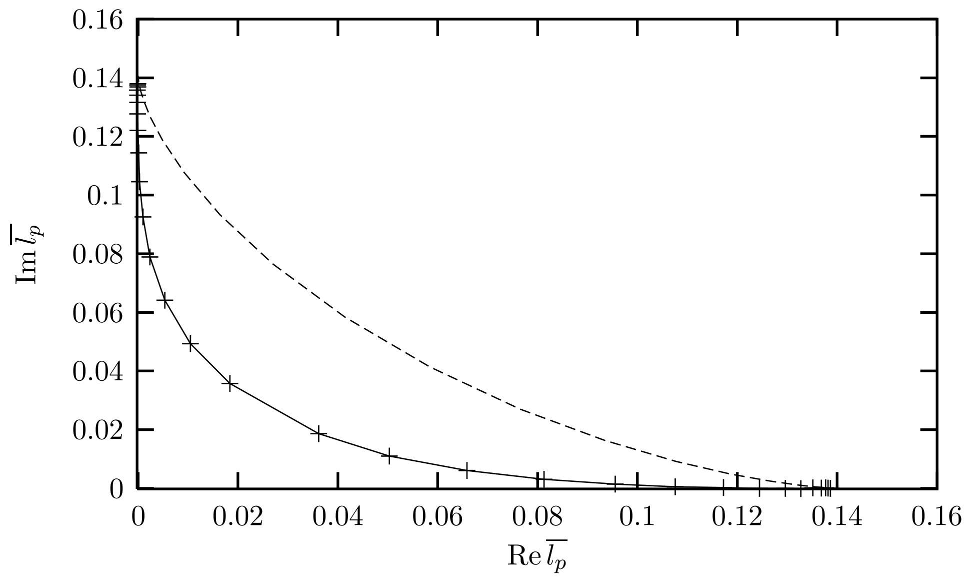

Figure 5: The values in the complex plane taken by the Polyakov loop for $x_3 \in [0, L-1]$, for the $k = 1$ wall in SU(4) with $aT = 0.25$ and $T \simeq 1.02T_c$. Dashed line is one-loop perturbation theory.

remarkably good down to $T \simeq 1.88T_c$. This implies that the shape of the relevant region of the effective potential remains close to the one-loop perturbative form, even at these low T. By contrast, once we descend very close to T_c, as in figure 5 at $T \simeq 1.02T_c$, the average locus has moved far from the one-loop curve suggesting that the effective action is now far from its high-T perturbative form. This observation makes it all the more remarkable that we continue to see Casimir Scaling at such very low T.

JHEP08(2005)060

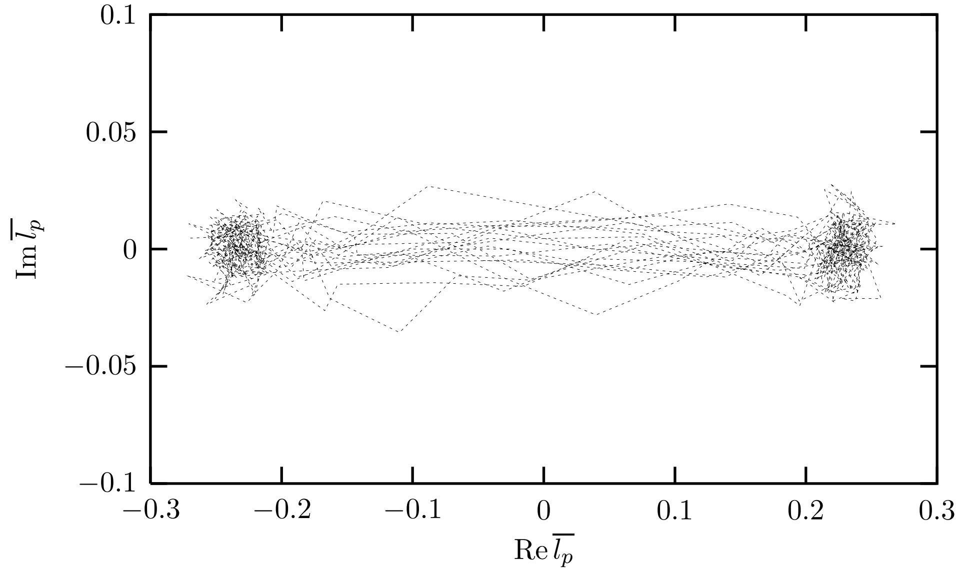

Figure 6: The values in the complex plane taken by the Polyakov loop for $x_3 \in [0, L-1]$ for a sample of individual $k = 2$ walls in SU(4) with $aT = 0.25$ and $T \simeq 1.88T_c$.

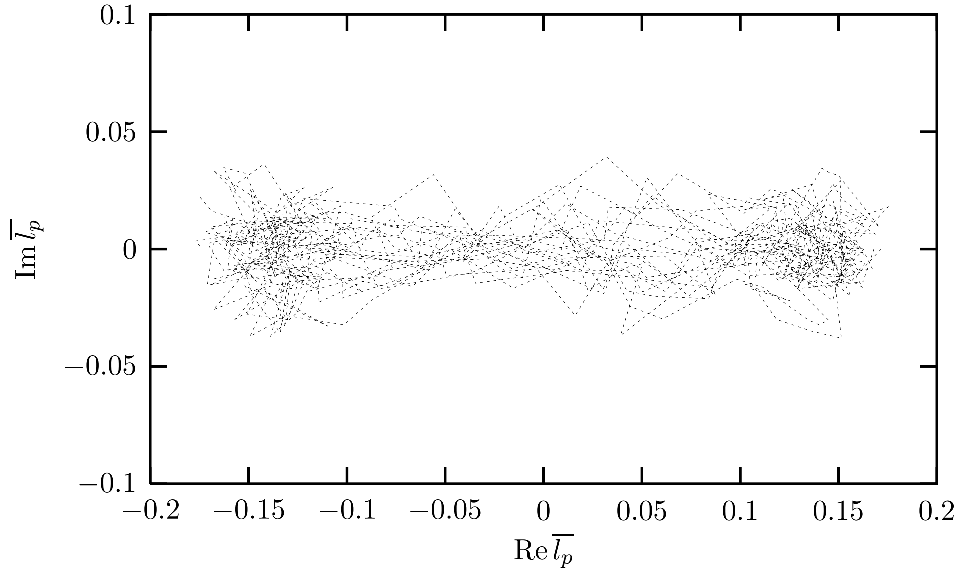

Figure 7: The values in the complex plane taken by the Polyakov loop for $x_3 \in [0, L-1]$ for a sample of individual $k = 2$ walls in SU(4) with $aT = 0.25$ and $T \simeq 1.02T_c$.

In SU(4) the average $k = 2$ wall profile between the $k = 0$ and $k = 2$ phases, must lie along the real axis by symmetry, just like the perturbative prediction. It is interesting to ask whether this is achieved by averaging over, say, two sets of tunnelling paths fluctuating around two degenerate minimum action paths, each away from the real axis, but which are related by $\mathrm{Im}\bar{l}_p \to -\mathrm{Im}\bar{l}_p$, or if there is only one such minimum tunnelling path, as in perturbation theory. In figure 6 and in figure 7 we show the loci for individual

JHEP08(2005)060

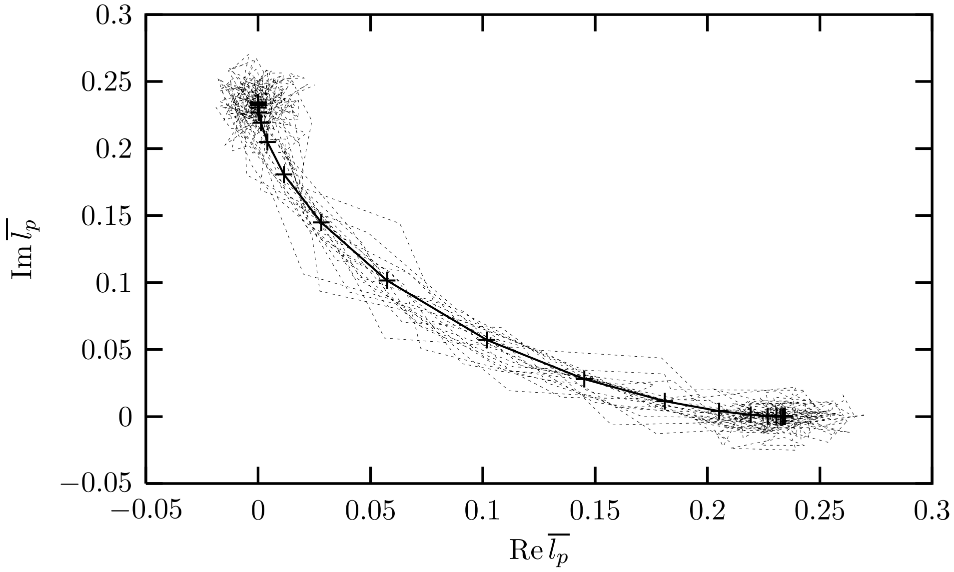

Figure 8: The values in the complex plane taken by the Polyakov loop for $x_3 \in [0, L-1]$ for a sample of individual $k = 1$ walls in SU(4) with $aT = 0.25$ and $T \simeq 1.88T_c$. Solid line is the average.

lattice fields containing a $k = 2$ wall, to illustrate that the latter is the case, both at $T \simeq 1.88T_c$ and at $T \simeq 1.02T_c$. Thus we can expect, as discussed in section 2.7, that the $k = N/2$ wall will indeed split into two confined-deconfined domain walls precisely at $T = T_c$.

It is also relevant to look at the corresponding plots for the $k = 1$ SU(4) wall. In figure 8 we show what happens at $T \simeq 1.88T_c$. More interesting is $T \simeq 1.02T_c$. We have seen in figure 5 that at this very low T the average locus is deformed so as to pass not very far from $\bar{l}_p = 0$. As we pointed out in section 2.7 we expect that as $T \to T_c$ there will be a second minimum action tunnelling path that passes along the real and imaginary axes near $\bar{l}_p = 0$, and which becomes the global minimum near T_c. Does the average in figure 5 include some paths that are tracing this alternative trajectory? In fact this appears not to be the case, at $T \simeq 1.02T_c$, as we see from figure 9. In the next section we shall see that at $T = T_c$ things do in fact become different.

As we have just seen, in practice the fluctuations are small enough that we can identify quite accurately the profile and hence the centre of the domain wall in each lattice field, at any of the above values of T. We can then translate that centre to a common value of x_3 and take an average over all the lattice fields so as to obtain the averaged domain wall profile. Let us relabel the position in the 3-direction by z, with the domain wall centered at $z = (L-1)/2$ and $z \in [0, L-1]$. In figure 10 we plot the average of the real part of the Polyakov loop as a function of z for the $L_0 = 4$ SU(4) calculation at $T \simeq 1.88T_c$. Note that for the $k = 1$ SU(4) wall the real part is not symmetric about the centre: one must exchange the real and imaginary parts. We do not show the imaginary part, to avoid cluttering the plot, but the same analysis and results follow in that case. We also show curves obtained using the one-loop formula in eqs. (2.21)–(2.25) with four different choices of coupling. Simply using the bare coupling $g^2 = 2N/\beta$ does not

JHEP08(2005)060

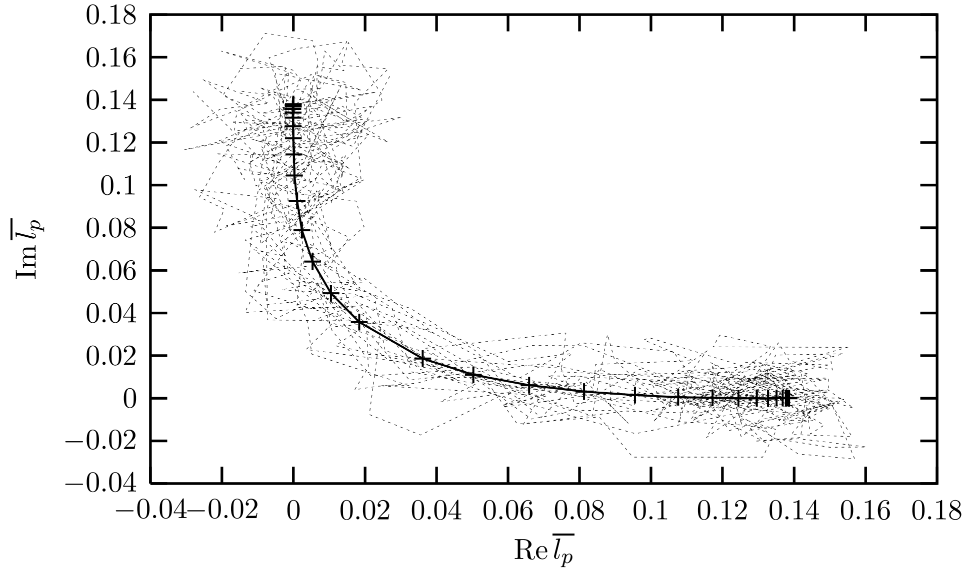

Figure 9: The values in the complex plane taken by the Polyakov loop for $x_3 \in [0, L-1]$ for a sample of individual $k = 1$ walls in SU(4) with $aT = 0.25$ and $T \simeq 1.02T_c$. Solid line is the average.

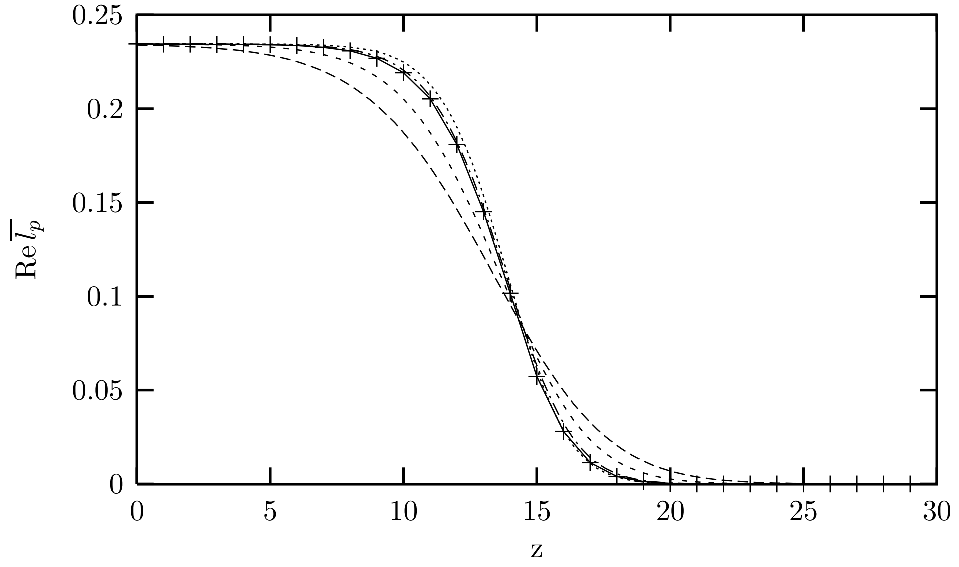

Figure 10: Solid line: the average of the real part of the Polyakov loop as a function of z for the $L_0 = 4$ SU(4) calculation at $T \simeq 1.88T_c$. One loop perturbative predictions using for $g^2(T)$ the lattice bare coupling (long dash), the mean field improved lattice coupling (short dash), the Schrödinger functional coupling (dot) and just a best fit (dash-dot).

reproduce the shape at all. The mean-field improved coupling defined in eq. (2.18) works better but not very well. The Schrödinger functional coupling discussed in appendix A works very well indeed. The last coupling, which is simply defined so as to minimise the discrepancy between the one-loop formula and the lattice result, works only slightly better than this.

JHEP08(2005)060

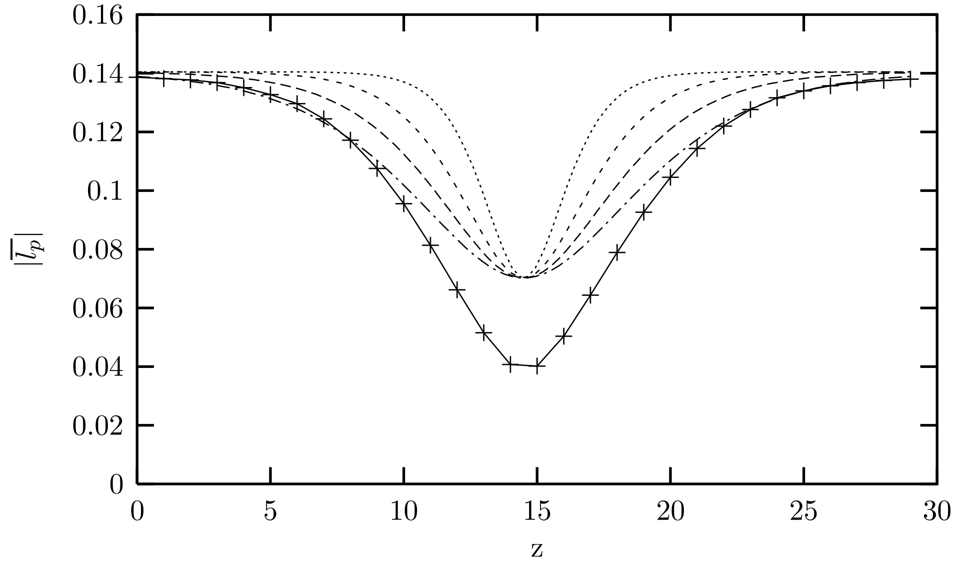

Figure 11: The average of the modulus of the Polyakov loop as a function of z for the $L_0 = 4$ SU(4) calculation at $T \simeq 1.02T_c$. One loop perturbative predictions using for $g^2(T)$ the lattice bare coupling (long dash), the mean field improved lattice coupling (short dash), the Schrödinger functional coupling (dot) and just a best fit (dash-dot).

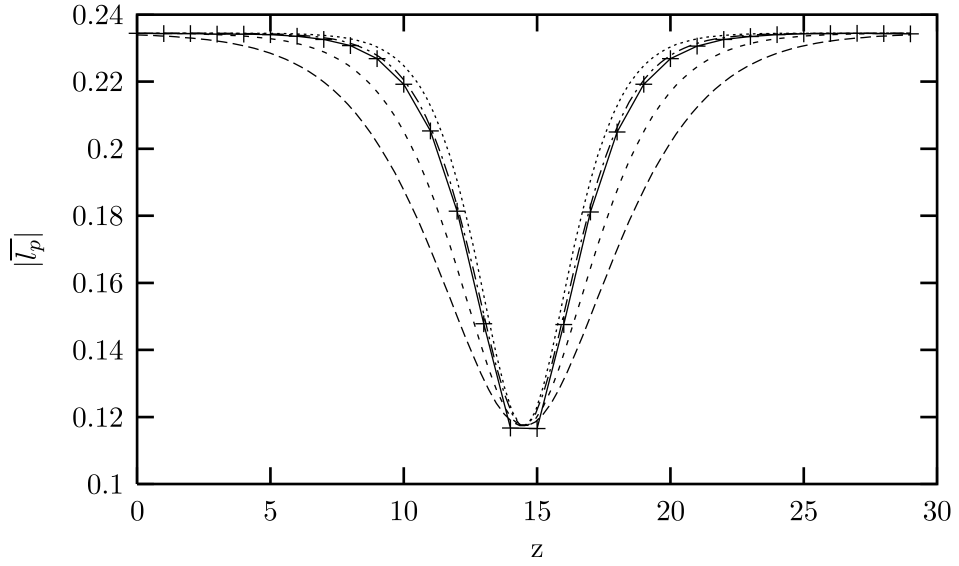

Figure 12: The average of the modulus of the Polyakov loop as a function of z for the $L_0 = 4$ SU(4) calculation at $T \simeq 1.88T_c$. One loop perturbative predictions using for $g^2(T)$ the lattice bare coupling (long dash), the mean field improved lattice coupling (short dash), the Schrödinger functional coupling (dot) and just a best fit (dash-dot).

At $T \simeq 1.02T_c$ we already know from figure 5 that no coupling will work well. We illustrate this in figure 11 where we plot the modulus of the Polyakov loop against z and compare it to the various perturbative predictions. Here we see the interesting feature that

JHEP08(2005)060

SU(4)			
β	T/T_c	$k=1$	$k=2$
10.497	1.016	no	no
10.494	1.012	no	no
10.491	1.007	mixed	flattens
10.488	1.002	mixed	mixed
10.485	0.998	splits	splits
10.482	0.993	splits	splits

Table 6: Behaviour of domain walls at $T \simeq T_c$ in SU(4).

SU(6)				
β	T/T_c	$k=1$	$k=2$	$k=3$
24.532	1.013	no	no	no
24.526	1.009	no	no	no
24.520	1.004	no	via origin	flattens
24.514	1.000	no	via origin	flattens
24.508	0.996	splits	splits	splits
24.502	0.991	splits	splits	splits

Table 7: As in table 6 but for SU(6).

the 'better' the coupling, the worse is its description of the profile. This is in contrast to what we find in figure 12 in a similar plot at $T \simeq 1.88T_c$. The reason for this is that the 'better' couplings are larger at lower T than the lattice bare coupling, and eq. (2.23) then predicts a thinner domain wall in lattice units (recalling that $T = 1/aL_0$ is fixed in lattice units). Here however the observed thickness of the wall actually grows as we lower T/T_c from 1.88 to 1.02. This would appear to contradict asymptotic freedom which tells us that $g^2(T)$ grows as $T \downarrow$ and hence, by eq. (2.23), that the wall narrows. This points to the fact that near T_c low-order perturbation theory is qualitatively, and not just quantitatively, unreliable. It is interesting to note that precisely the same phenomenon is found [5] to occur for the lightest mass that couples (strongly) to the Polyakov loop. (At high T this is just twice the electric screening mass m_D.) As we see from eq. (2.12), we would expect m_D to approach its high-T linear behaviour from above since $g^2(T)$ decreases with T; however lattice calculations show that the approach is from below [5]. Since $1/m_D$ is the natural length scale for the thickness of the domain wall, this observation ties in with what we have found here.

3.3 Wetting

Motivated by the discussion in section 2.7, we have performed a set of calculations extremely close to $T = T_c$. They are not intended to be accurate enough to provide a useful estimate of ΔS; rather we wish to see if the k-wall separates into two cd walls at $T \simeq T_c$ in a Monte Carlo sequence of several thousand field configurations. We perform such calculations for $k = 1, 2$ walls in SU(4) on a $4 \times 100 \times 20^2$ lattice and for $k = 1, 2, 3$ walls in SU(6) on a $5 \times 100 \times 20^2$ lattice. We use long lattices so that if a k-wall breaks up into two cd walls there is enough space for two well separated walls.

Our observations are summarised in table 6 and table 7. The first thing we note is that the transition from no sign of wetting to the complete splitting of the domain walls takes place over a very small range of T which is precisely around $T = T_c$. (See eq. (3.1).) For $k \neq N/2$ we first have a profile that is well away from the origin ('no'). Then at lower T we typically see fluctuations of the wall profile which deform it so that it sometimes passes through the origin ('via origin') but does not visibly break up. If we lower T further the wall fluctuates more strongly, so that the profile not only goes through the origin, but

JHEP08(2005)060

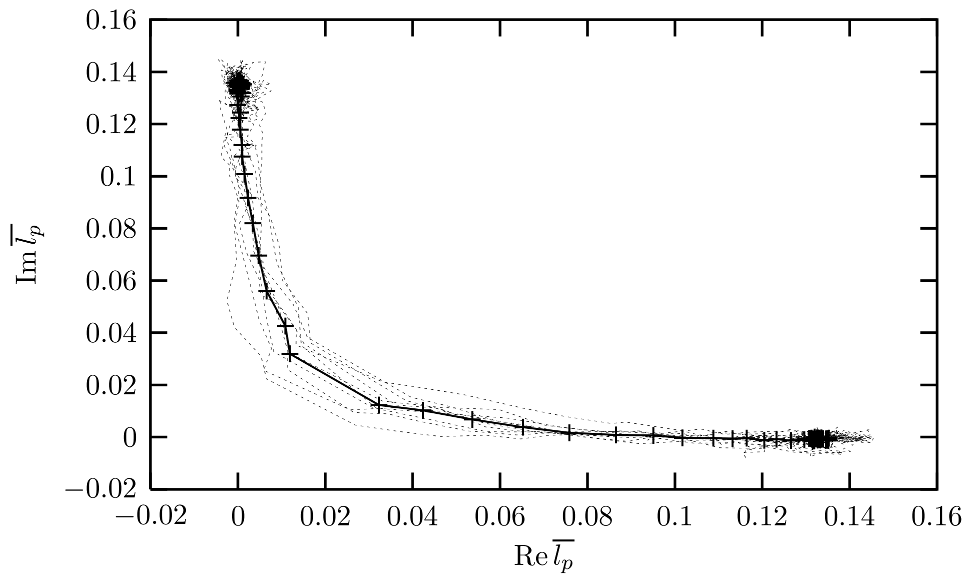

Figure 13: The values in the complex plane taken by the Polyakov loop for $x_3 \in [0, L-1]$ for a sample of $k = 1$ walls in SU(4) at $\beta_c = 10.491$, i.e $T \simeq 1.006T_c$. The lines represent averages over subsequences of 100 sweeps, taken over the first 1000 sweeps.

the wall splits, reforms, and again reassumes a profile well away from the origin ('mixed'). Finally, at lower T still, the k-wall splits completely ('splits'). All this takes place over an interval $\delta T/T_c \sim 0.005$. For the $k = N/2$ walls not all these stages are identifiable because the profile normally passes through the origin. But a precurser to the separation, a central 'flattening', can be identified and presumably overlaps with the 'via origin' and 'mixed' stages for $k \neq N/2$.

It is interesting to ask what happens to the $k = 1$ SU(4) profile, shown in figure 9 for $T \simeq 1.02T_c$, when we lower the temperature to $T \simeq T_c$. To illustrate this we show in figure 13 a set of 10 profiles obtained over a sequence of 1000 Monte Carlo sweeps and in figure 14 over a later sequence of 1000 sweeps, all at $T \simeq 1.006T_c$. Each locus has been obtained by averaging over subsequence of 100 field configurations. We observe that the domain walls in figure 13 have profiles that fluctuate around an average locus that is similar to the one we saw in figure 8. The profiles in figure 14, on the other hand, fluctuate around a quite different locus that passes through $\bar{l}_p = 0$ and which is identical to the minimum $k = 2$ path up to the $\pi/2$ rotation at the origin. What we appear to see is a tunnelling between these two paths and this strongly suggests that the effective potential has two minimal paths separated by a ridge through which the system has to tunnel. Once it has tunnelled to the set of paths passing through $\bar{l}_p = 0$ it will readily split into two cd walls at $T = T_c$. One would expect that the surface tension of the $k = 1$ and $k = 2$ walls that pass through $\bar{l}_p = 0$ will be approximately the same rather than being related by Casimir Scaling. The statistics of our calculations near $T = T_c$ do not allow a direct test of this reasonable conjecture.

We observe that, within our resolution, the wetting of the SU(4) $k = 2$ and $k = 1$ walls appears to occur simultaneously and it appears to occur at $T = T_c$. This would appear to tell us that $\sigma_W^k(T_c) \not< 2\sigma_{cd}(T_c)$ for both $k = 1$ and $k = 2$ at $N = 4$. For SU(6) there is

JHEP08(2005)060

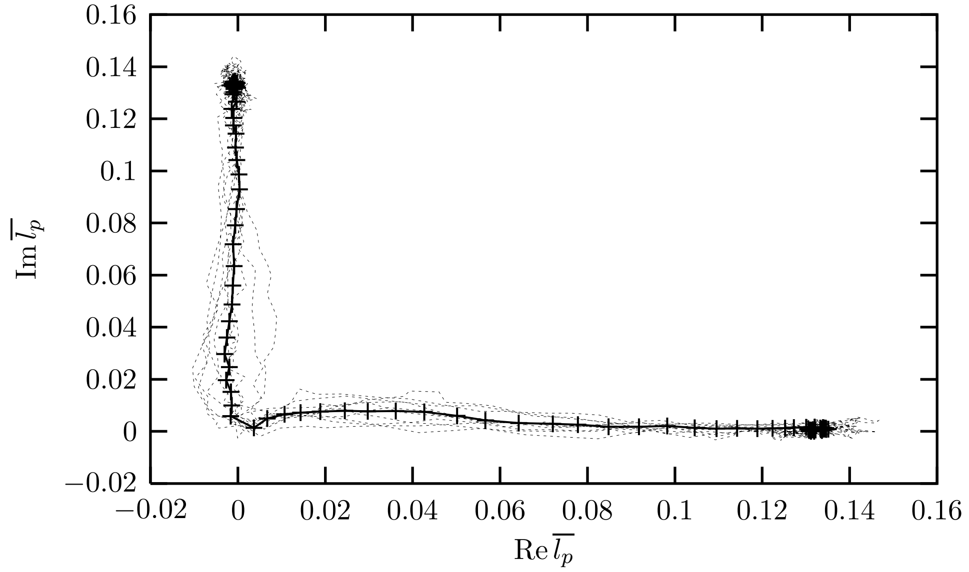

Figure 14: As in the previous figure, but for a later sequence of 1000 sweeps.

perhaps some evidence that the $k = 2$ and $k = 3$ walls begin to split slightly before the $k = 1$ wall. If this hint were to survive a more careful calculation, then we would have the beginnings of a calculation of the N-dependence of σ_{cd} as oulined earlier.

The fact is that all the k-walls appear to break up at almost the same value of T again raises the question whether this can be consistent with the k-wall tensions being different and related by Casimir Scaling as $T \to T_c$, since in that case it is clear that one would expect the higher-k walls to split at a higher T than the lower-k walls.

To address this question and also to understand why everything occurs in such a very narrow range of T around T_c, we need to look at the magnitudes of the quantities involved. First consider the 'natural' magnitude of σ_W^k near $T = T_c$ as given by the one loop part of eq. (2.1) and using a realistic coupling. Plugging in the value that the Schrödinger functional coupling takes at T_c in SU(3), $g(T_c) \simeq 2.2$ and assuming $g^2(T_c)N$ is constant, we obtain

$$\sigma_W^k(1 - \text{loop}) = k(N-k)\frac{4\pi^2}{3\sqrt{3}}\frac{T_c^3}{\sqrt{g^2(T)N}} \simeq 2k(N-k)T_c^3\,. \tag{3.4}$$

We now compare it to the latent heat [5]

$$\frac{L_h}{T_c} \simeq 0.35N^2T_c^3 + O(\frac{1}{N^2})\,. \tag{3.5}$$

It is natural to compare L_h divided by T_c to σ_W^k because the latter is a free energy per unit area that is effectively integrated over the thickness of the wall, which is $O(1/T_c)$. We observe from eq. (3.4) that for the maximal wall, $k = N/2$, $\sigma_W^k(1-\text{loop}) \simeq 0.5N^2T_c^2$ and this is of the same order as the value of L_h/T_c. This seems reasonable, given that there is one scale in the problem. Now consider σ_{cd}. Although, as we have emphasised, it is not known if it increases as N^2, such a fit is certainly possible, and one then finds [5]

$$\sigma_{cd} \simeq (0.014N^2 - 0.104)T_c^3\,. \tag{3.6}$$

JHEP08(2005)060

This is very small compared to the previous two quantities; e.g. for SU(4) it is about a factor of 50 smaller than L_h/T_c. The reason for this mismatch between these two energy scales is not entirely clear (but see below). Nonetheless, as we shall now argue, it is what leads to the onset of wetting occuring over such a narrow range of T around T_c.

To be explicit we consider the SU(4) calculation with $L_0 = 4$. As we have seen in figure 3 the actual value of σ_W^k drops well below the one-loop value in eq. (3.4) once $T \leq 2T_c$ and it collapses to a value consistent with zero as $T \to T_c$. Nonetheless we have seen that neither of the k-walls shows any sign of splitting into two cd walls even at $T \simeq 1.02T_c$. This is also true even closer to T_c, as shown in table 6, but the relevant runs are much shorter there. Consider first the $k = 2$ wall. Consider a fluctuation just above T_c in which it breaks up into two cd walls separated by a region of confining phase. For this region of confining phase to be clearly distinguishable, it needs to be of some minimal size, presumably $O(1/T_c)$ long. Assuming (as we have argued above) that $\sigma_W^{k=N/2} \simeq 2\sigma_{cd}$ at and near T_c, the probability of such a fluctuation will simply be due to the free energy cost, ΔF_{cd}, of the region of confining phase. Approximating this by the latent heat, L_h, multiplied by the area A and the length $1/T_c$, one has a suppression

$$\propto \exp\left\{-\frac{L_h A}{T T_c}\left\{1 - \frac{T_c}{T}\right\}\right\} \overset{T \simeq T_c}{\simeq} \exp\left\{-\frac{L_h}{T_c^4}\frac{L_1 L_2}{L_0^2}\left\{1 - \frac{T_c}{T}\right\}\right\}. \tag{3.7}$$

Plugging in the value for L_h/T_c^4 in eq. (3.5) and $L_1 = L_2 = 5L_0$ we see that the range of T/T_c in which such wetting fluctuations have a significant probability is very small and on the order of

$$\frac{T - T_c}{T_c} \leq \frac{1}{140}. \tag{3.8}$$

Consider now a $k = 1$ wall in our SU(4) calculation. We do not know enough about its dynamics to analyse the situation precisely, but we can outline a plausible scenario within which we can see why the splitting takes place very close to T_c. (The splitting essentially refers to the tunnelling exemplified in figure 13 and figure 14.) If the $k = 2$ wall splits into two cd walls at $T = T_c$ we have $\sigma_W^{k=N/2}(T_c) = 2\sigma_{cd}(T_c)$ and if we also have Casimir Scaling then $\sigma_W^{k=1}(T_c) = 4/3 \times \sigma_{cd}(T_c)$. and the $k = 1$ wall will not split at $T = T_c$ but only at a lower T where the free energy advantage of a layer of confining phase provides the required extra $2/3 \times \sigma_{cd}(T_c)$ needed for splitting. Assuming a region of confining phase of length $O(1/T_c)$ and neglecting the variation with T of both $\sigma_W^{k=1}$ and σ_{cd} leads to an estimate for the T where the $k = 1$ wall splits of

$$\frac{T_c - T}{T_c} \sim \frac{2}{3}\frac{\sigma_{cd}}{L_h/T_c} \sim 0.013 \tag{3.9}$$

using eq. (3.6) and eq. (3.5). This is a very crude estimate, of course, but it serves to illustrate how the large ratio of the energy scales associated with L_h/T_c and σ_{cd} mean that the difference between the values of T at which the $k = 2$ and $k = 1$ walls break up is, assuming Casimir Scaling, very small and on the order of the resolution of our calculations. That is to say, our calculations do not in fact provide evidence against Casimir Scaling persisting at all T (until the walls break up). A similar argument will explain why the

JHEP08(2005)060

process of breaking up occurs over a very narrow range of T around T_c. It also implies that any attempt to verify dynamical 'perfect wetting' must have an extremely fine resolution in T near T_c, and particularly so for SU(3) where the ratio $L_h/T_c\sigma_{cd}$ is even larger.

We have ignored the fact that both σ_{cd} and $\sigma_W^{k=1}$ will vary with T. This variation, as T moves away from T_c, is likely to be driven by the growing free energy difference between the two phases and so is likely again to be on the order of $L_h/T_c \times (T - T_c)/T_c$, in which case we will obtain a result similar to the one above. Of course, as we move away from T_c either way, we will eventually encounter the spinodal point at which one or both types of wall ceases to exist.

We briefly return to the question why $\sigma_{cd}(T_c)$ is so small compared to L_h/T_c. At $T = T_c$ there is a cancellation of differences in entropy and internal energies between the confined and deconfined phases. Nonetheless one might have expected the 'hills' and 'passes' in the effective potential at$T = T_c$ to have a natural scale of $O(L_h)$. This would imply a value for $\sigma_W^k(T_c)$ and $\sigma_{cd}(T_c)$ that is $O(L_h/T_c)$, which is consistent with low-order perturbation theory, but not with what we actually find to be the case. Clearly our expectation is mistaken: the 'passes' are also strongly suppressed. As we move a little away from T_c the free energy density difference between the phases increases roughly like $\sim L_h|1 - T/T_c|$. The behaviour of the domain walls suggests that the whole effective potential, not just the wrong vacuum, scales something like this: $\sigma_{cd}(T_c)$ and $\sigma_W^k(T_c)$ are small because the height of the 'pass' which the tunnelling path traverses is also small — presumably the same dynamics as the free energy cancellation. As we move away from T_c the height of the pass also grows roughly as $\sim L_h|1-T/T_c|$. This suggests that $\sigma_W^k(T)$ will grow in this way as T increases above T_c — qualitatively in accord with what we see in figure 3.

This might also suggest a scenario in which both $\sigma_{cd}(T)$ and $\sigma_W^k(T)$ have a minimum at $T = T_c$ but this requires the effective potential to be very similar in shape above and below T_c (with just the depth of the minima reversed) which hardly seems likely.

The fact that the k-walls do break up only at $T \simeq T_c$ does tell us that σ_W^k cannot be very much larger than $2\sigma_{cd}$ once we are very near to $T = T_c$. This confirms the strong suppression of σ_W^k indicated in figure 1. We note that this appears to be an effect that survives the $N \to \infty$ limit and provides further evidence that even in that limit the deconfined phase is far from being a weakly coupled gluon plasma in the region from T_c to several times T_c. This fits in with the observation that the SU(3) pressure anomaly is also a large-N effect [27].

3.4 't Hooft string condensation

The fact that $\sigma_W^k(T)$ decreases rapidly towards a value that is close to zero, as we decrease T towards T_c, tells us that the spatial 't Hooft string tension, $\tilde{\sigma}_k(T) = \sigma_W^k(T)/T$, also decreases.

Since the deconfining transition is robustly first order (for larger N) we can use its metastability to discuss what happens in the deconfined phase for at least some range of temperatures $T < T_c$. Doing so, the observed rapid decrease suggests that $\tilde{\sigma}_k = 0$ at some temperature $T_{\tilde{H}}$ that is close to and below T_c. This suggests that as we decrease T in the deconfined phase, then at $T = T_{\tilde{H}}$ we would encounter a second-order phase transition

JHEP08(2005)060

driven by the condensation of spatial 't Hooft strings — if it were not for the intervening presence of the first order transition to the (more-or-less) separate confining ensemble of energy eigenstates of the theory.

This is reminiscent of the expectation that as one increases T within the confining phase, there would be a second order Hagedorn-like string condensation transition at $T = T_H$, if it were not, once again, for the intervening presence of the first order transition to the (more-or-less) separate 'gluon gas' ensemble of energy eigenstates of the theory. Indeed one can use the metastability of this first order transition to obtain direct evidence for this would-be second order transition and to estimate its location at $T = T_H > T_c$, as has been done in [28].

The condensation of confining strings as $T \to T_H^-$, leads to deconfinement, but without reference to the 'gluon plasma'. Similarly one can see how the condensation of (spatial) 't Hooft strings as $T \to T_{\tilde{H}}^+$, leads to confinement, but without reference to the usual confining phase. As the domain wall tension goes to zero, the vacuum will break down into a gas of bubbles containing different Z_N phases so that the Polyakov loop, $\bar{l}_p$, is zero.

All this hints at some kind of a duality between the confined and deconfined phases.

4. Conclusions

We have shown in this paper that the surface tensions of the domain walls separating different deconfined phases in the euclidean formulation of finite-T SU(N) satisfy Casimir Scaling, i.e.

$$\sigma_W^k = k(N-k)\, f\left(g^2(T)N, \frac{T}{T_c}\right) T^3\,, \tag{4.1}$$

to a good approximation. We have shown this to be the case not only at very high T where our calculations of $\partial\sigma_W^k/\partial T$ merely reproduce the perturbative predictions [1, 2], but all the way down to $T \simeq 1.02T_c$ where, not surprisingly, both the wall profile and the magnitude of the surface tension are very far from perturbation theory. It appears that the Casimir Scaling predicted by low-order perturbation theory is in fact a much more general property of these domain walls and, equivalently, the spatial 't Hooft string tension.

Our numerical results are for $\partial\sigma_W^k/\partial T$ rather than for σ_W^k itself, but we can interpolate the former and integrate it so as to estimate the T dependence of the latter. We have too few values of $\partial\sigma_W^k/\partial T$ to be able to do so with any precision, however the striking qualitative feature is that as we reduce T below, say, $2T_c$ the surface tension becomes strongly suppressed relative to its perturbative value, reaching values close to zero at $T \simeq T_c$.

We have also performed calculations near and passing through T_c. Here, in a very narrow range of temperatures around T_c, we see all the k-walls splitting into confined-deconfined walls. The fact that the Polyakov loop profiles of $k = N/2$ domain walls are found to pass through zero, at any T, (almost) inevitably leads to the 'perfect wetting' at $T = T_c$ of such walls. The reason that all the k-walls 'wet' at values of T very close to T_c, is intimately linked with the fact that the latent heat, which provides a measure of how the confining-deconfining free energy difference increase with $T - T_c$, is very much larger than the surface tension, σ_{cd}, of the confined-deconfined domain wall. This means that to test

JHEP08(2005)060

ideas of ‘perfect wetting’ for $k \neq N/2$ domain walls, e.g. the usual domain walls in SU(3), will require calculations with a very fine resolution in T — certainly finer than ours, and quite possibly finer than any previous calculations.

There are a number of ways in which our calculations could be usefully improved upon. Firstly, the comparison with perturbation theory would be under much better control if we were to have two-loop calculations of σ_W^k in the various coupling schemes that we have tried. Turning to our lattice calculations, while these do allow us some control of the continuum limit and the large-N limit, it is clear that in both respects our calculations could be significantly, and usefully, improved upon. Calculations at more values of T would transform our very crude reconstruction of the value of $\sigma_W^k(T)$ into something much more controlled and credible. In addition it would be very useful to analyse the Polyakov loop profiles, and hence the effective action, not just in terms of the trace, but in terms of the fuller range of gauge invariant variables provided by the eigenvalues of the Polyakov loop. This would allow us to transform our plausible inferences into strict derivations (or the opposite, as the case may be).

We have noted that the rapid decrease of both $\sigma_W^k(T)$ and the spatial ’t Hooft string tension, $\tilde{\sigma}_k(T) = \sigma_W^k(T)/T$, as we decrease T towards T_c, suggests the presence of what would be a second order phase transition a little below T_c if it were not for the intervening presence of the first order transition. This is reminiscent of the conjecture that as one increases T within the confining phase, the condensation of confining strings would occur, a little above T_c, if it were not, once again, for the intervening presence of the first order transition. Just as has been done in the latter case [28] it would be interesting to use the metastability of the first order transition to go beyond T_c for direct evidence of the second order transition. It would also be very interesting to perform the sort of calculations we have done, but more densely in T, so as to determine the functional form of $\tilde{\sigma}_k(T)$ much more reliably and precisely. This would help us to explore the possibility of a duality between the behaviours as $T \to T_H^-$ and $T \to T_{\tilde{H}}^+$.

Acknowledgments

Our lattice calculations were carried out on PPARC and EPSRC funded computers in Oxford Theoretical Physics. FB acknowledges the support of a PPARC graduate studentship.

A. Schrödinger functional coupling

When $T \to T_c$ the coupling $g^2(T)$ becomes large and our choice of the mean-field improved coupling evaluated at $a = 1/L_0T$, i.e. $g_I^2(a)$, may become inadequate. To estimate the range of uncertainty introduced by this choice, we calculate the perturbative expression for the wall tension in section 2.4 with a ‘good’ coupling at the scale $T^{-1} = aL_0$.

We need a coupling that has been explicitly calculated to length scales that are quite large. For this purpose we shall use the calculation in [19]. This calculation is for SU(3) and we shall therefore perform our analysis for $N = 3$. The coupling in [19] has been

JHEP08(2005)060

extrapolated to the continuum limit, but we shall apply it to a finite a, assuming the corrections are insignificant for our purposes.

The running of the coupling $\bar{g}$ in [19] is given by

$$-l\frac{\partial \bar{g}}{\partial l} = \beta(\bar{g}) = -b_o\bar{g}^3 - b_1\bar{g}^5 - b_2^{\text{eff}}\bar{g}^7 \tag{A.1}$$

where

$$b_0 = 11(4\pi)^{-2}\,, \qquad b_1 = 102(4\pi)^{-4}\,, \qquad b_2^{\text{eff}} = 1.5(8)(4\pi)^{-3}\,. \tag{A.2}$$

(Here b_2^{eff} is a fitted effective coefficient that subsumes higher order corrections and is not intended to be an estimate of the coefficient b_2 of the β-function in this coupling scheme.) The normalisation of the coupling is then fixed by its value at the largest length scale at which it is calculated

$$\bar{g}^2(l_m) = 3.48\,; \qquad l_m = 4a(\beta_0 = 5.904)\,. \tag{A.3}$$

This length scale is $l_m \simeq 2/3T_c$ which is not quite as large as we would like but is large enough that extrapolating it to $l = 1/T_c$ might be qualitatively reliable.

Defining the reduced length

$$\hat{l} = \frac{l}{l_m} \tag{A.4}$$

we solve eqs. (A.1), (A.2) numerically, with the boundary condition of eq. (A.3), so obtaining $\bar{g}^2(\hat{l})$ for any desired value of $\hat{l}$. The quantity that appears in eq. (2.16) and which we now need to evaluate is

$$\frac{\partial}{\partial\beta}\frac{1}{\bar{g}(\hat{l})} = -\frac{1}{\bar{g}^2(\hat{l})}\frac{\partial\bar{g}(\hat{l})}{\partial\hat{l}}\frac{\partial\hat{l}}{\partial\beta}\,. \tag{A.5}$$

We will perform the calculation for a lattice with $L_0 = 4$ and with varying $T = 1/a(\beta)L_0$. So we evaluate the coupling at

$$\hat{l} = \frac{l}{l_m} = \frac{L_0 a(\beta)}{L_0 a(\beta_0)} = \frac{a\sqrt{\sigma}(\beta)}{a\sqrt{\sigma}(\beta_0)}\,. \tag{A.6}$$

We now use the expression for $a\sqrt{\sigma}(\beta)$ as a function of β that is provided in table 5 of [5] for the range $5.6925 \leq \beta \leq 6.338$, to evaluate both $\hat{l}$ in eq. (A.6) and $\partial\hat{l}/\partial\beta$ in eq. (A.5) in this range of β. (Like any multi-parameter interpolation, this cannot be assumed to be useful outside the range in which it was fitted.)

We now have all the ingredients to calculate each of the factors on the rhs of eq. (A.5). The first factor comes by plugging in the calculated value of $\hat{l}$ into the numerically determined $\bar{g}^2(\hat{l})$. The second factor is just the β-function in eq. (A.1) evaluated with this $\bar{g}^2(\hat{l})$. To obtain the third factor one differentiates the interpolating formula in table 5 of [5] and evaluates it at the desired value of β, and normalises it to the formula at $\beta_0 = 5.904$. Since $T_c = 1/4a(\beta_c)$ for $\beta_c = 5.6924(2)$ [25] and this lies within our interpolation range, we are able to perform this calculation down to $T = T_c$. To transform this coupling to one for SU(4) we simply assume that g^2N is fixed at fixed T.

We use the above in the formulae of section 2.4 and show in figure 1 the resulting value for $\Delta S_W/L_1L_2$ of the 2-loop perturbative wall tension using the coupling $\bar{g}^2(T^{-1} = aL_0)$.

JHEP08(2005)060

We also show the values obtained with the mean-field improved coupling, $g_I^2(a)$, and the unimproved bare coupling, $g^2(a)$. Finally we show the values obtained from the lattice simulation. We observe that the more realistic the coupling, the closer the perturbative value moves towards the lattice values. However a substantial discrepancy remains, strongly suggesting at $T \simeq T_c$ the domain wall can no longer be usefully described within perturbation theory.

References

[1] T. Bhattacharya, A. Gocksch, C. Korthals Altes and R.D. Pisarski, *Interface tension in an* $\mathrm{SU}(N)$ *gauge theory at high temperature*, *Phys. Rev. Lett.* **66** (1991) 998; *Z(n) interface tension in a hot* $\mathrm{SU}(N)$ *gauge theory*, *Nucl. Phys.* **B 383** (1992) 497 [hep-ph/9205231]; P. Giovannangeli and C.P. Korthals Altes, *'t Hooft and Wilson loop ratios in the QCD plasma*, *Nucl. Phys.* **B 608** (2001) 203 [hep-ph/0102022].

[2] P. Giovannangeli and C.P. Korthals Altes, *'t Hooft and wilson loop ratios in the QCD plasma*, *Nucl. Phys.* **B 608** (2001) 203 [hep-ph/0102022]; *Spatial 't Hooft loop to cubic order in hot QCD, II*, hep-ph/0412322.

[3] C. Korthals Altes, A. Michels, M.A. Stephanov and M. Teper, *Domain walls and perturbation theory in high temperature gauge theory:* $\mathrm{SU}(2)$ *in* $2+1$ *dimensions*, *Phys. Rev.* **D 55** (1997) 1047 [hep-lat/9606021].

[4] D.J. Gross, R.D. Pisarski and L.G. Yaffe, *QCD and instantons at finite temperature*, *Rev. Mod. Phys.* **53** (1981) 43.

[5] B. Lucini, M. Teper and U. Wenger, *Properties of the deconfining phase transition in* $\mathrm{SU}(N)$ *gauge theories*, *JHEP* **02** (2005) 033 [hep-lat/0502003].

[6] J. Ambjørn, P. Olesen and C. Peterson, *Stochastic confinement and dimensional reduction, 1. Four-dimensional* $\mathrm{SU}(2)$ *lattice gauge theory*, *Nucl. Phys.* **B 240** (1984) 189; *Stochastic confinement and dimensional reduction. 2. three- dimensional* $\mathrm{SU}(2)$ *lattice gauge theory*, *Nucl. Phys.* **B 240** (1984) 533; *Three-dimensional lattice gauge theory and strings*, *Nucl. Phys.* **B 244** (1984) 262; *Observation of a string in three-dimensional* $\mathrm{SU}(2)$ *lattice gauge theory*, *Phys. Lett.* **B 142** (1984) 410; S. Deldar, *Static* $\mathrm{SU}(3)$ *potentials for sources in various representations*, *Phys. Rev.* **D 62** (2000) 034509 [hep-lat/9911008]; G.S. Bali, *Casimir scaling of* $\mathrm{SU}(3)$ *static potentials*, *Phys. Rev.* **D 62** (2000) 114503 [hep-lat/0006022].

[7] B. Lucini and M. Teper, *The* $k=2$ *string tension in four dimensional* $\mathrm{SU}(N)$ *gauge theories*, *Phys. Lett.* **B 501** (2001) 128 [hep-lat/0012025]; *Confining strings in* $\mathrm{SU}(N)$ *gauge theories*, *Phys. Rev.* **D 64** (2001) 105019 [hep-lat/0107007].

[8] L. Del Debbio, H. Panagopoulos, P. Rossi and E. Vicari, *K-string tensions in* $\mathrm{SU}(N)$ *gauge theories*, *Phys. Rev.* **D 65** (2002) 021501 [hep-th/0106185]; *Spectrum of confining strings in* $\mathrm{SU}(N)$ *gauge theories*, *JHEP* **01** (2002) 009 [hep-th/0111090].

[9] Ph. de Forcrand, B. Lucini and M. Vettorazzo, *Measuring interface tensions in 4d* $\mathrm{SU}(N)$ *lattice gauge theories*, hep-lat/0409148.

[10] B. Lucini, M. Teper and U. Wenger, *Glueballs and k-strings in* $\mathrm{SU}(N)$ *gauge theories: calculations with improved operators*, *JHEP* **06** (2004) 012 [hep-lat/0404008].

JHEP08(2005)060

[11] G. 't Hooft, *On the phase transition towards permanent quark confinement*, *Nucl. Phys.* **B 138** (1978) 1; *A property of electric and magnetic flux in nonabelian gauge theories*, *Nucl. Phys.* **B 153** (1979) 141.

[12] J. Greensite, *The confinement problem in lattice gauge theory*, *Prog. Part. Nucl. Phys.* **51** (2003) 1 [hep-lat/0301023].

[13] A. Hart, B. Lucini, Z. Schram and M. Teper, *Vortices and confinement in hot and cold* $D = 2 + 1$ *gauge theories*, *JHEP* **06** (2000) 040 [hep-lat/0005010].

[14] M. Srednicki and L. Susskind, SU(5) *monopoles on the lattice*, *Nucl. Phys.* **B 179** (1981) 239.

[15] A. Hart, B. Lucini, Z. Schram and M. Teper, Z_2 *monopoles in* $D = 2 + 1$ SU(2) *lattice gauge theory*, *JHEP* **11** (2000) 043 [hep-lat/0010010].

[16] C.P. Korthals Altes, *Forces, fluxes and quasi-particles in hot QCD*, hep-ph/0308229;
A. Kovner, *Confinement, magnetic* Z_N *symmetry and low-energy effective theory of gluodynamics*, hep-ph/0009138; *Magnetic* Z_N *symmetry in 2+1 dimensions*, *Int. J. Mod. Phys.* **A 17** (2002) 2113 [hep-th/0211248].

[17] G. Parisi, *Recent progress in gauge theories*, in *High Energy Physics* - 1980 (AIP 1981);
G.P. Lepage and P.B. Mackenzie, *On the viability of lattice perturbation theory*, *Phys. Rev.* **D 48** (1993) 2250 [hep-lat/9209022];
G.P. Lepage, *Redesigning lattice QCD*, hep-lat/9607076.

[18] F. Di Renzo, E. Onofri and G. Marchesini, *Renormalons from eight loop expansion of the gluon condensate in lattice gauge theory*, *Nucl. Phys.* **B 457** (1995) 202 [hep-th/9502095].

[19] M. Lüscher, R. Sommer, P. Weisz and U. Wolff, *A precise determination of the running coupling in the* SU(3) *Yang-Mills theory*, *Nucl. Phys.* **B 413** (1994) 481 [hep-lat/9309005].

[20] Y. Iwasaki, K. Kanaya, L. Karkkainen, K. Rummukainen and T. Yoshie, *Interface tension in quenched QCD*, *Phys. Rev.* **D 49** (1994) 3540 [hep-lat/9309003].

[21] M. Laine and Y. Schroder, *Two-loop QCD gauge coupling at high temperatures*, *JHEP* **03** (2005) 067 [hep-ph/0503061];
M. Laine, *What is the simplest effective approach to hot QCD thermodynamics?*, hep-ph/0301011.

[22] B. Lucini and M. Teper, SU(N) *gauge theories in 2+1 dimensions: further results*, *Phys. Rev.* **D 66** (2002) 097502 [hep-lat/0206027];
M.J. Teper, SU(N) *gauge theories in 2+1 dimensions*, *Phys. Rev.* **D 59** (1999) 014512 [hep-lat/9804008].

[23] M. Teper, *The finite temperature phase transition of* SU(2) *gauge fields in (2+1)-dimensions*, *Phys. Lett.* **B 313** (1993) 417;
J. Engels et al., *A study of finite temperature gauge theory in (2+1) dimensions*, *Nucl. Phys.* **53** *(Proc. Suppl.)* (1997) 420 [hep-lat/9608099].

[24] J. Liddle and M. Teper, in progress.

[25] B. Lucini, M. Teper and U. Wenger, *The high temperature phase transition in* SU(N) *gauge theories*, *JHEP* **01** (2004) 061 [hep-lat/0307017].

[26] Z. Frei and A. Patkos, *Perfect wetting: an alternative for hadronic matter formation in the cooling universe*, *Phys. Lett.* **B 229** (1989) 102.

JHEP08(2005)060

[27] B. Bringoltz and M. Teper, in preparation.

[28] B. Bringoltz and M. Teper, in preparation.

JHEP08(2005)060